Calcium phosphate bioceramics: From cell behavior to chemical-physical properties

Amandine Magnaudeix

frontiers | Frontiers in Biomaterials Science

TYPE Review
PUBLISHED 30 August 2022
DOI 10.3389/fbiom.2022.942104

OPEN ACCESS

EDITED BY
Regine Willumeit-Römer,
Helmholtz Center Hereon, Germany

REVIEWED BY
Livia Santos,
Nottingham Trent University,
United Kingdom
Giuseppe Pezzotti,
Kyoto Institute of Technology, Japan

*CORRESPONDENCE
Amandine Magnaudeix,
amandine.magnaudeix@unilim.fr

SPECIALTY SECTION
This article was submitted to Bio-interactions and Bio-compatibility, a section of the journal Frontiers in Biomaterials Science

RECEIVED 12 May 2022
ACCEPTED 21 July 2022
PUBLISHED 30 August 2022

CITATION
Magnaudeix A (2022), Calcium phosphate bioceramics: From cell behavior to chemical-physical properties.
Front. Front. Biomater. Sci. 1:942104.
doi: 10.3389/fbiom.2022.942104

Calcium phosphate bioceramics: From cell behavior to chemical-physical properties

Amandine Magnaudeix*

Univ. Limoges, CNRS, Institut de Recherche sur Les Céramiques, UMR 7315, Limoges, France

Calcium phosphate ceramics, including hydroxyapatite (HA), have been used as bone substitutes for more than 40 years. Their chemical composition, close to that of the bone mineral, confers them good biological and physical properties. However, they are not sufficient to meet all the needs in bone regenerative medicine, such as in the context of critical bone lesions. Therefore, it is essential to improve their biological performances in order to extend their application domains. In this aim, three approaches are mainly followed on the assumption that the biological response can be tuned by modifications of the chemical physical properties of the ceramic: 1) Incorporation of specific chemical species into the calcium phosphate crystalline lattice of chemical elements to stimulate bone repair. 2) Modulation of the bioceramic architecture to optimize the cellular responses at the interface. 3) Functionalization of the bioceramic surface with bioactive molecules. These approaches are supposed to act on separate parameters but, as they are implemented during different steps of the ceramic processing route, they cannot be considered as exclusive. They will ineluctably induces changes of several other physical chemical properties of the final ceramic that may also affect the biological response. Using examples of recent works from our laboratory, the present paper aims to describe how biology can be affected by the bioceramics modifications according to each one of these approaches. It shows that linking biological and chemical physical data in a rational way makes it possible to identify pertinent parameters and related processing levers to target a desired biological response and then more precisely tune the biological performance of ceramic biomaterials. This highlights the importance of integrating the biological evaluation into the heart of the processes used to manufacture optimized biomaterials.

KEYWORDS

calcium phosphate bioceramics, hydroxyapatite, chemical-physical properties, bone tissue, functionalization

Introduction

The repair of critical bone lesions is a major clinical difficulty and a societal public health issue (Wang and Yeung, 2017; Ho-Shui-Ling et al., 2018). According to the diamond concept, the prerequisites for bone healing consist of a mechanically stable environment (matrix), the presence of osteogenic cells (precursors or stem cells), an

osteoconductive matrix on the surface of which bone cells can adhere, proliferate and differentiate, and an osteoinductive stimulus (Giannoudis et al., 2007). Therefore, the ideal implanted material should be biocompatible, osteoconductive and osteoinductive (i.e., a material able to stimulate the recruitment and differentiation of precursors into mature bone cells). Moreover, vascularisation is an essential condition for bone tissue repair (Calori and Giannoudis, 2011; Mercado-Pagán et al., 2015). It allows on the one hand the oxygenation of the tissue, the elimination of metabolic waste products and the supply of certain cellular precursors able of homing. On the other hand, through the transport of biologically active molecules (growth factors and cytokines), it contributes to the mechanisms of cellular communication involving cells that belong to different systems (immune, vascular, bone) that are necessary to the proper sequencing of the cascade of cellular events leading to bone healing. Trabecular (or cancellous) bone autograft (or autologous bone graft) consists in transplanting a highly porous structure (50%–90% interconnected porosity), portion of trabecular bone taken from a healthy donor site of the patient himself. Rapidly vascularised, osteoconductive, osteoinductive and containing osteogenic cells, bone autograft, with superior biological properties, remains the gold standard. But it has significant limitations related to the amount, size and poor mechanical properties of the available graft, and it induces additional morbidity for the patient (Brydone et al., 2010; Wang and Yeung, 2017; Tang et al., 2021). Thus, the use of autologous graft is not or hardly possible for the repair of large size bone lesions for which the self-repair properties of bone are not sufficient. Synthetic bone substitutes are a major alternative to autografts. In this context, calcium phosphate ceramics are widely used in bone tissue repair for their excellent biocompatibility and osteoconductive properties. Amongst them, synthetic hydroxyapatite (HA, $Ca_{10}(PO_4)_6(OH)_2$) has a chemical composition close to that of the natural bone mineral which consists of a carbonated apatitic phase associated with mineral ions and trace elements in non-apatitic environments (Combes et al., 2016; Rey and Combes, 2016) with the following approximated formula: $Ca_{8,3}(PO_4)_{4,3}(HPO_4,CO_3)_{1,7}(CO_3,OH)_{0,3}$ (Legros et al., 1987; Rey et al., 2009). Several steps are needed to produce HA ceramics (summarized in Figure 1). First, the raw powder is synthesized, usually, by the means of an aqueous precipitation route at low temperature (Raynaud et al., 2002; Palard et al., 2008) or by solid state reaction at high temperature (Rao et al., 1997). Then, in a second step, the powder is shaped to obtain a 3D green part. Various methods can be used to this end among which emerging CAD/CAM additive manufacturing technologies such as (micro)stereolithography or robocasting. These last ones are of high interest to shape 3D ceramic scaffolds with complex architectures suitable for on-demand medicine (Champion et al., 2017; Marchat and Champion, 2017; Charbonnier et al., 2021). At last, in a third step, the shaped body is sintered at high temperature, typically around 1,200°C for HA ceramics. This thermal treatment, performed at a temperature lower than the melting (or decomposition) point, allows for solid state diffusion of chemical species inducing consolidation and densification of the green part to obtain the final ceramic part (Champion, 2013). A debinding step at intermediate temperature (around 500°C) prior to sintering can be necessary in the case of a parts shaped with organic additives to remove them by burning.

Shaped as porous scaffolds, HA-based ceramics can be colonised by neo-formed bone tissue after implantation. Interconnected macropores from 300 to 600 µm in diameter are described to have the ideal size to favour vascularization and tissue penetration in bone substitutes (Karageorgiou and Kaplan, 2005; Hutmacher et al., 2007). In this regard, hydroxyapatite was successfully used in particular clinical contexts such as cranial implant to rehabilitate large cranial bone defects (Brie et al., 2013). However, bone tissue regeneration is limited to small volumes so that the colonisation within the implanted device hardly extends deeper than about 1 cm from bone apposition. One of the reasons given is that the vascular invasion of the implant is too low, limiting the supply of nutrients and oxygen, which impedes cell survival (Marchat and Champion, 2017), which restricts the possibilities for bone reconstruction (discussed in Marchat and Champion, 2017). Consequently, while excellent results, HA-based bioceramics are not suitable for number of applications in bone repair. Amongst reasons for a limited in-depth tissue/cell colonization is the poor vascularization of such scaffolds and a limited diffusion of nutrients and oxygen that impedes cell survival (Marchat and Champion, 2017).

Numerous strategies are currently investigated to enhance bone regeneration by modifying one or several chemical-physical properties of calcium phosphate ceramics to improve their biological properties. These strategies acts on several identified levers that are associated with the fabrication steps of a ceramic biomaterial (Figure 1). The first one is the ceramic chemical composition, which can be tuned during the initial step of powder synthesis by incorporating elements of biological interest in the HA crystal lattice. The release of potentially chemotactic chemical species may enable the material to actively recruit bone progenitors cells. They may also stimulate other cellular activities such as differentiation and be cell type specific. The second mean of action consists of adjusting the scaffold architecture at different scales since cells and tissues are very sensitive to their microenvironment, notably to the material surface topography (Skoog et al., 2018). Here, shaping with additive manufacturing processes allows to master the design of macropores with controlled size (typically in the range 300–800 µm) and geometry. Moreover, controlling the sintering parameters (Champion, 2013), makes it possible to adjust the microporosity (size <10 µm), thereby increasing the specific surface area, surface roughness and total surface energy, and thus influencing the cell behavior at the biomaterial surface

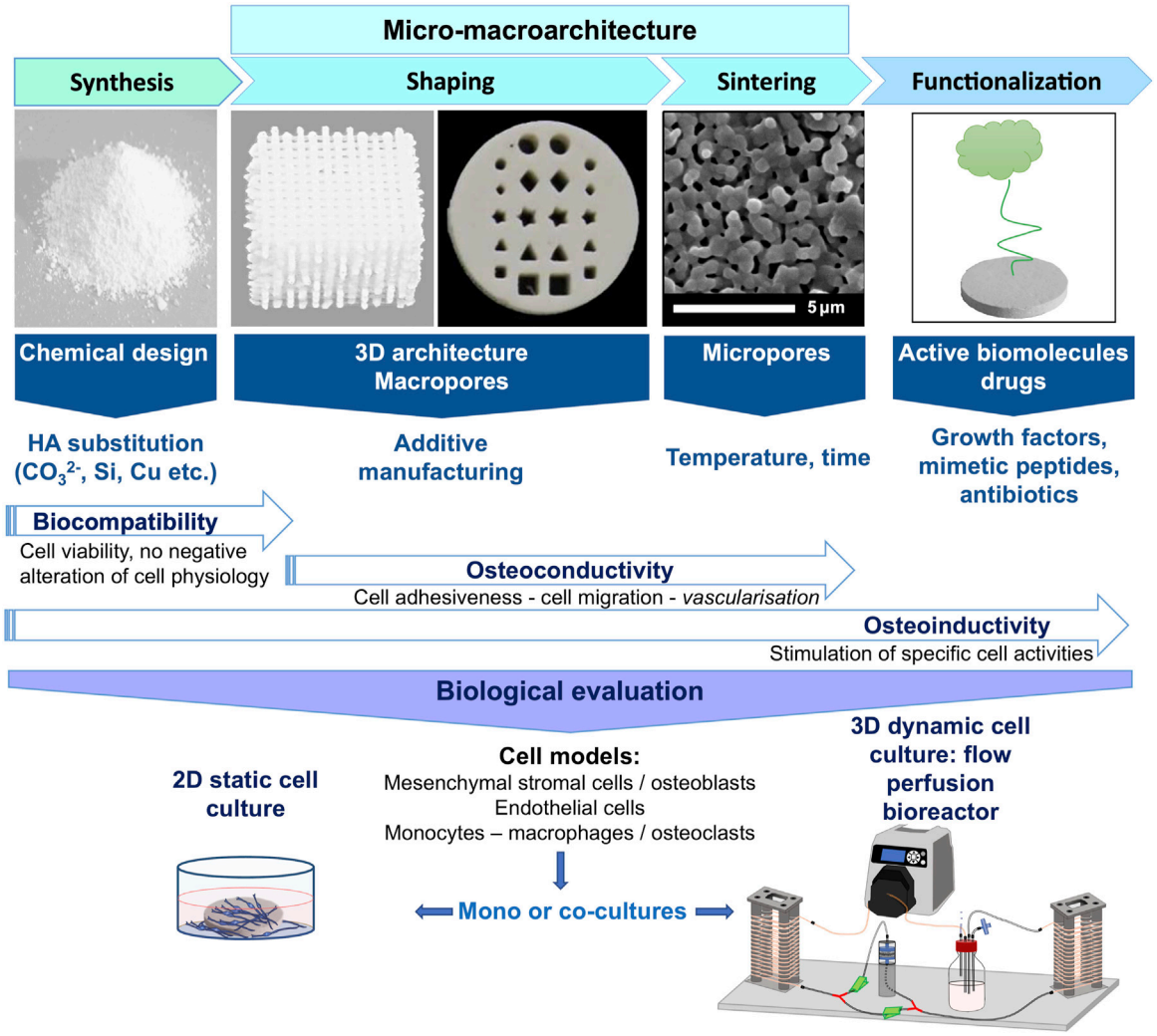

FIGURE 1
Synthesis scheme of the different steps necessary to elaborate hydroxyapatite-based ceramics for bone tissue engineering, from the powder synthesis to the evaluation of its biological properties. Each strategy that can be followed to enhance the bioceramic biological properties, i.e., HA substitution, tuning of its micro-macro-architecture and functionalization by active biomolecules or drugs, are indicated according to the fabrication step at which it can be applied. Such interventions on ceramic chemical-physical properties affect its biological properties in terms of biocompatibility, osteoinductivity and/or osteoinductivity. These biological properties are evaluated using relevant cellular models more or less complex, i.e. by the use of mono-culture or co-culture of cell lines involved in the bone repair process, either in 2D static conditions, or in 3D dynamic condition under perfusion flow which is more realistic and relevant to understand the biomaterial/living interfaces.

(Gariboldi and Best, 2015). Finally, once the ceramic is produced, it is possible to functionalize it with active (bio)molecules or cells (Hench and Polak, 2002; Damia et al., 2021).

Whatever the followed strategy, obviously an important point is the evaluation of the final bioceramic applicative performances using appropriate biological models *in vitro* and *in vivo*. Depending of the problematic, several choices have to be managed accurately. For example, *in vitro*, the choices are based the one hand on the culture method, from 2D static set up to 3D dynamic flow perfusion culture, and on the other hand, on the cellular model, from immortalized cell line monocultures to primary cell line co-cultures (Champion et al., 2017) (Figure 1). The present paper illustrates the strategies developed in our research team to improve HA bioceramics biological properties by acting on their chemical-physical properties during the fabrication steps (Figure 1). It shows how biology can be affected through some of our published results focused on HA ceramics. These examples don't only highlight the importance of biological evaluations as final step of a biomaterial development but also how, when integrated in the ceramic elaboration process, they help to rationalize it.

TABLE 1 Examples of HA substitution with substitution site and empirical chemical formulas.

Substituting element	Substituted element	Substitution site	General chemical formula	References
SiO_4^{4-}	PO_4^{3-}	PO_4 group	$Ca_{10}(PO_4)6_{-x}(SiO_4)_x(OH)_{2-x}$	Palard et al. (2008)
Cu^+/Cu^{2+}	H^+	OH group	$Ca_{10}(PO_4)_6Cu_z^{II}Cu_y^{I}O_2H_{2-2z-y}$ ($y \gg z$)	Bazin et al. (2021)
CO_3^{2-}	PO_4^{3-}	PO_4 group (B type)	$Ca_{10-x}(PO_4)_{6-x}(CO_3)_x(OH)_{2-x}$	Lafon et al. (2008)
	OH^-	OH group (A type)	$Ca_{10}(PO_4)6(OH)_{2-2x}(CO_3)_x$	
	PO_4^{3-} and OH^-	Mixed (A/B type)	$Ca_{10-x}(PO_4)_{6-x}(CO_3)_x(OH)_{2-x-2y}(CO3)_y$	

The examples given in this table are to put in regard with substituted HA ceramics discuted in part 2.2.

Tuning HA-based bioceramics chemical composition

Principles of ionic substitutions

As exposed above, one of the most common strategies employed to enhance the biological properties is to incorporate substituting metal or trace elements in the crystal lattice of HA (Bose et al., 2013).

HA crystal belongs to the crystallographic family of apatites characterized by a general formula $Me_{10}(XO_4)_6(Y)_2$, where Me is a divalent cation, XO_4 a trivalent anionic group and Y a monovalent anionic group. Thus, in the case of HA, Me is calcium, XO_4, the phosphate group and Y is a hydroxyl ionic group. HA is defined by a Ca:P molar ratio of 10:6, a hexagonal crystal structure with lattice parameters a = b = 9.432 Å, c = 6.881Å and angle β = 120°. The apatite structure is particularly favourable to accept ionic substitutions or vacancies (Elliott, 1994; Šupová, 2015). Table 1 gives some examples that are in regard with the substituted HA ceramics described throughout the following sections. Cations are most often incorporated in place of Ca^{2+}. This is the case for example of Sr^{2+} or Mg^{2+} giving $Ca_{10-x}A_x(PO_4)_6(OH)_2$ where A is the substituting element. The case of copper is special since it may have several oxidation degrees. Amongst works on copper-substituted HA production, incorporation of Cu^{2+} cations at the Ca site of HA was described with the theoretical resulting formula: $Ca_{10-x}Cu_x(PO_4)_6(OH)_2$. (Shanmugam and Gopal, 2014; Othmani et al., 2018). Some recent works argue in favour of a incorporation of copper with mixed valence states (Gomes et al., 2018). We have demonstrated that Cu substitutes H^+ cations in the hexagonal channel of HA lattice, with a majority of monovalent Cu^+ cations while minor substitution by divalent Cu^{2+} likely exists, resulting in the following empiric formula: $Ca_{10}(PO_4)_6Cu_z^{II}Cu_y^{I}O_2H_{2-2z-y}$ ($y \gg z$) (Bazin et al., 2021) (Table 1). Anionic groups, such as SiO_4^{4-} can replace either PO_4 group (usually named as B site or B type substitution). In this case, the charge balance imposes the creation of anionic vacancies in the OH site (named as A site). In the case of carbonate CO_3^{2-}, the substitution can take place either in the A or B or mixed A/B site depending on the synthesis route and/or sintering procedure (Table 1). Here also, the charge balance leads to presence of vacancies in both the Ca and OH sites for B type carbonate substitution and to OH vacancies for a A type substitution.

Most of the time, the doping elements are chosen because they exist as trace elements in the biological apatite which constitutes the natural bone mineral (Elliott, 1994). They are expected to influence positively bone repair due to their intrinsic biological effects. Strontium, silicon and manganese would stimulate osteoblast activity, the bone forming cells, whereas copper or cobalt are intended to have a positive effect on endothelial cells, the master actors of angiogenesis (Bose et al., 2013; O'Neill et al., 2018). Additional properties, such as an antibacterial effect, are also addressed in order to prevent the risk of infection that can occur after implantation of a bone substitute. For this application, silver and copper are the most investigated elements to dope HA (Zhao et al., 2022).

Consequences for HA ceramic properties

As pointed out by the literature, chemical substitutions in HA alter also its mechanical, chemical and physical properties (grain size, surface energy, wettability, solubility. . .) (Bose et al., 2013; Šupová, 2015; Ratnayake et al., 2017). In turn, these alterations may greatly affect the biology of cell and tissues at the material/living interface. In this respect, HA carbonatation is a strategy to increase the too low solubility of HA and thus, enhance its bioactivity (Lafon et al., 2008; Pieters et al., 2010). Finally, for a given introduced ionic species, many sources of variation appear, due to the material elaboration by itself, or/and to the methods of physical, chemical and biological characterizations that are implemented. As a result, data from the literature are not consensual and not comparable. The following examples illustrate this statement.

We successfully produced HA substituted bioceramics, respectively by carbonate ions (Lafon et al., 2008) or copper ions (Bazin et al., 2021), and tested *in vitro* some features of their biological properties (Germaini et al., 2017; Bazin et al., 2021). In the case of copper (Bazin et al., 2021), CuHA bioceramics were produced by solid-state reaction sintering at 1,100°C. The Cu/Ca ratio ranged from 0.01 to 0.07. Copper was inserted in the HA crystal lattice mainly as Cu^+ cation substituting for H^+ in OH channels. The preliminary biological assays conducted using MC3T3-E1 pre-osteoblastic cells, directly cultivated onto bioceramics surface for

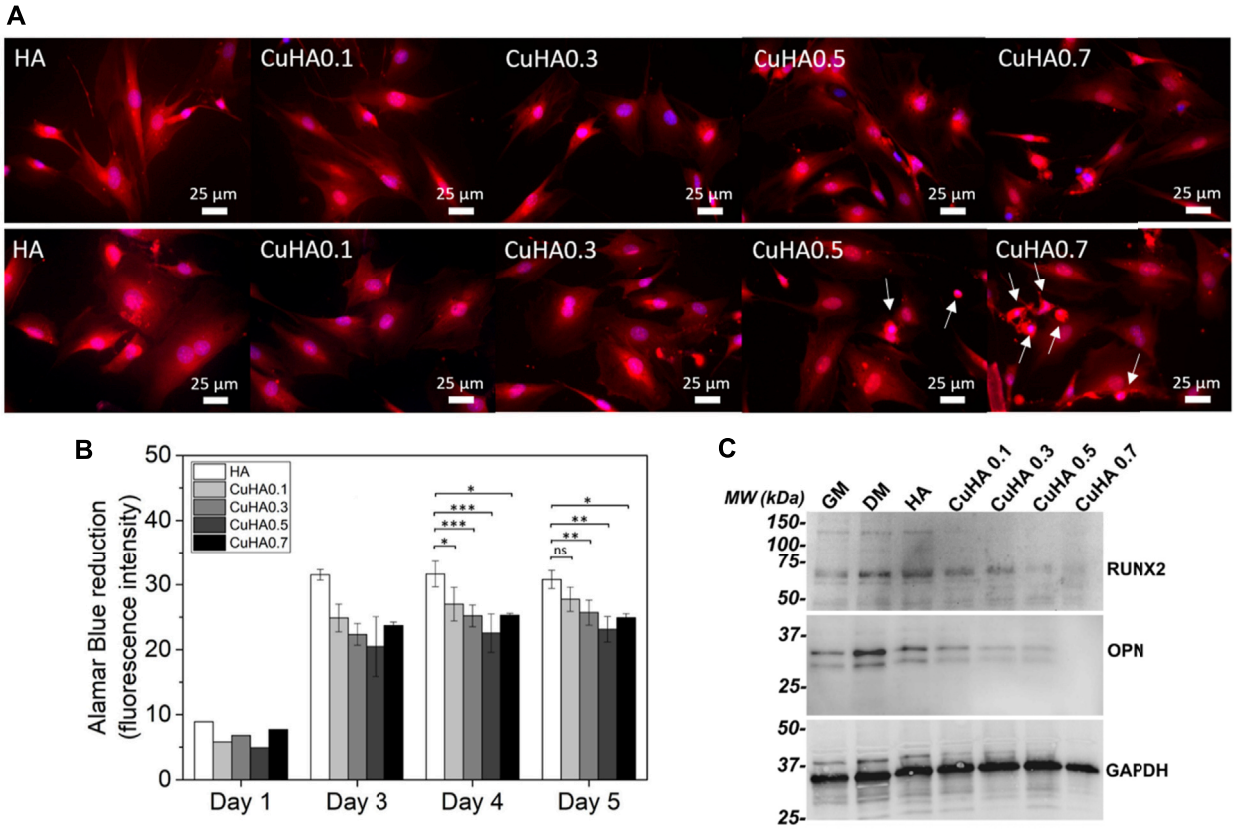

FIGURE 2
In vitro evaluation of copper-doped hydroxyapatite bioceramics properties on MC3T3-E1 murine pre-osteoblasts. **(A)** Morphology of the viable cells observed in fluorescence microscopy after staining with calcein red-orange (in red); the nuclei were stained with Hoescht 33342 (in blue) after 3 days (upper panel) and 5 days (lower panel) of culture, arrows indicate cells presenting an apoptotic morphology. **(B)** Metabolic activity of the cell population over time evaluated by Alamar Blue assay. Statistical analysis: ANOVA-One way followed by Tukey post-hoc test: ns: non significant; *: $p < 0.05$; **: $p \leq 0.01$; ***: $p \leq 0.0001$. **(C)** Western-blot evaluation of the expression of RUNX2 and OPN in MC3T3-E1 cells. Adapted from Ceramics International, 47, Tiphaine Bazin, Amandine Magnaudeix, Richard Mayet, Pierre Carles, Isabelle Julien, Alain Demourgues, Manuel Gaudon, Eric Champion, Sintering and biocompatibility of copper-doped hydroxyapatite bioceramics, Pages No. 13644–13654, Copyright (2022), with permission from Elsevier.

5 days showed a good biocompatibility of the ceramics towards these cells for a copper content up to 3.4%wt (Figure 2A). A reduction of cell growth (Figure 2B) and a negative effect on osteogenic differentiation (Figure 2C) were detected whatever the copper content might be. We are currently working on a more thorough evaluation of the biological properties of these ceramics using endothelial cells. First results have shown that the presence of copper in HA lattice stimulates endothelial cells proliferation and acts positively on the expression of PECAM-1, a marker of endothelial cell activation (Brunel et al., 2021).

At the time of the publication of this work, only few studies performed biocompatibility tests on copper-doped HA materials (Li et al., 2010; Gomes et al., 2018). Differences in the material elaboration methods on the one hand, and on the applied biological procedures and models on the other hand have returned strong divergences in the results from biocompatibility evaluations. For the same Cu/Ca = 0.01 M ratio, copper-substituted HA pellets obtained from an ion exchange method were cytotoxic after 1 day of incubation (Li et al., 2010). In this case, the copper-substituted HA was not sintered so likely highly reactive, and a B-type CO_3 substitution in HA was also found, which should induce a higher material solubility compared to uncarbonated HA. In the work by Gomes et al., biphasic pellets (HA containing 1.4 wt% of tricalcium phosphate as secondary phase) calcined at 1,200°C were found to be biocompatible after 1 week of culture (Gomes et al., 2018). The work from Hui et al. (2020), showed a biocompatibility of extracts from sintered HA hollow spheres containing copper on a murine cell line of bone stromal precursors. However, from the available data, it is not possible to have an idea of the copper amount in the system (Hui et al., 2020). Therefore, the chemical structure, the secondary phases as well as the microstructure of the tested copper substituted HA materials likely influence the biocompatibility to a great extent.

Another notable point is that different biological models were used: human fetal fibroblast in Li et al., human mesenchymal stromal cells (MSC) in the work of Gomez et al., and murine MC3T3-E1 pre-osteoblasts in our study (Li et al., 2010; Gomes et al., 2018; Bazin et al., 2021). Beyond the biological interest and mode of action by which copper influences cell physiology, it is worth noting that, in the case of eukaryotic cells, the toxicity thresholds of copper in solution differs greatly depending of the cell lines. An optimal positive effect, while not globally osteogenic (no effect in growth medium), was shown on human MSC around 100 µM of Cu^{2+} in the culture medium. But, copper became rapidly toxic when doses increased. A MSC inhibition was detected from 300 µM of Cu^{2+} in solution. In this case, copper was released from deposits made galvanically on titanium (Burghardt et al., 2015). Schamel et al., have described that MSC tolerate about 250 µM of copper without impairment of their proliferation (Schamel et al., 2017). In another study, a dose of 0.7 µM of copper was enough to reduce by 50% rat MSC viability after 3 days of culture (Li et al., 2019). This result contrasts with another work dealing with the effect of copper in solution on rat MSC where the toxicity threshold of copper was found above 10 µM while non-toxic dose inhibited osteogenic differentiation (Li et al., 2014). A toxicity was detected for copper in solution from a dose of 111 µM of copper in solution for murine MC3T3-E1 pre-osteoblasts. Human Umbilical Vein Endothelial Cells (HUVEC) were more resistant with a toxicity beginning from a double concentration (222 µM) (Li et al., 2019). The copper toxicity threshold has been found around 10 µM for peripheral blood mononucleated cells (PBMC) cultured in osteoclastic differentiation medium and above 20 µM for differentiated osteoclasts. Moreover an inhibition of the osteoclast resorption activity was found for non-toxic copper doses when copper was added during the process of osteoclastic differentiation of the cells; mature osteoclasts being less sensitive at these doses (Bernhardt et al., 2021).

Some concerns about the reproducibility of results are also raised concerning calcium phosphate bioceramics dissolution in biological fluids which depends not only on the chemical changes, but also on the surface topography. Carbonatation of HA, by increasing the material solubility and hence its biodegradability, is sought to increase the biological performance and osteointegration of carbonated HA bone substitutes in comparison with pure HA. In this context, after having successfully produced 4.4 wt% A/B carbonated-HA ceramics of chemical formula $Ca_{9.5}(PO_4)_{5.5}(CO_3)_{0.5}(OH)(CO_3)_{0.25}$ from works of Lafon et al., the objective of one of our study aimed at relating its chemical-physical properties to its biological properties using stoichiometric (pure) HA ceramic as a reference material (Lafon et al., 2008; Germaini et al., 2017). Being known the importance of the equilibrium in the activity of bone forming cells (osteoblasts) and bone-degrading cells (osteoclasts) for bone homeostasis, cell lines representative of these two cell types were used in this study, respectively MC3T3-E1 murine pre-osteoblasts and RAW264.7 monocytic cell line cultured in presence of osteoclastogenic proteins (M-CSF and RANKL). It is also known that for a given chemical or physical parameter, e.g., surface topography, cells from different types do no react necessary in the same way. For example, in connection with their very close microenvironment, osteoblasts and osteoclasts are not stimulated by the same roughness level (Costa et al., 2013). Thus, the bioceramics used in this study were manufactured to be as comparable as possible for this physical feature. They were microporous and had the same total amount of open microporosity (around 25%), which was obtained by tuning the sintering parameters (temperature, time, atmosphere) (Lafon et al., 2008; Champion, 2013). Results of chemical-physical characterizations of both HA and carbonated HA materials are presented in Table 2.

Murine pre-osteoblast cells adhered similarly on both surfaces (pure and carbonated HA ceramics). Carbonated HA stimulated pre-osteoblast proliferation but did not favored osteogenic differentiation in comparison with HA (Figures 3A–D). The murine mononucleated monocyte cell line RAW 264.7 was cultivated in osteoclastic differentiation medium at the surface of both ceramics. Here again both materials were biocompatible, allowing both differentiation of RAW 264.7 monocytes into osteoclast-like cells without toxicity (measured using WST-8 and LDH assays) or impairment of proliferation (evaluated by means of an ELISA dosage of BrdU incorporation into dividing cells). Carbonated HA showed an ability to stimulate osteoclast-like cell metabolism without stimulating significantly their differentiation. Interestingly, the resorption lacuna observed by SEM after lysis of cells were very different from one material to the other (Figures 3E,F). The calcium amount in the liquid medium surrounding the bioceramics, in the presence of cells or without cells, was dosed. This permitted to show that the carbonatation of HA efficiently increased its bioresorbability by two mechanisms: 1) increasing the HA solubility as depicted by the setup of a dissolution-precipitation equilibrium (with or without osteoblast and without osteoclast-like cells); 2) stimulating the material resorption by osteoclast-like cells. In conclusion of this study, 4.4 wt% of carbonate leads to an adapted concentration of calcium in the fluid surrounding the ceramic to stimulate both osteoblast and osteoclast cells activity, inducing a particularly interesting balance between biodegradation and osteogenesis to favor bone regeneration. It worth to note here that cell density, proliferation and metabolic activity were tested separately. This allowed to reveal that a greater number of cells (in the case of osteoclast-like cells) was not correlated to the metabolic activity usually assayed in order to test viability or proliferation. This justifies that in any case results from a metabolic activity test should be discussed with respect to the experimental settings and the other biological data to be conclusive.

A drawback of carbonate substitution of HA is the thermal instability making its sintering at high temperature difficult to handle without decomposition. In order to solve this problem on the one hand and to produce bioceramics with chemistry closer

TABLE 2 Chemical and physical properties of sintered pellets (n: number of independent measurements).

	HA	CHA
Chemical composition	$Ca_{10}(PO_4)_6(OH)_2$ Ca/P = 1.667 ± 0.002 (n = 3)	$Ca_{9.5}(PO_4)_{5.5}(CO_3)_{0.5}(OH)(CO_3)_{0.25}$ carbonate content: 4.43 ± 0.03w% (n = 3) Ca/P = 1.73[a]
Zeta potential (mV)	−25 ± 5	−22 ± 4
Specific surface area (m^2/g)	4.0 ± 0.3 (n = 4)	1.4 ± 0.1 (n = 4)
Porosity (%)	25.0 ± 0.6 (n = 8)	25.0 ± 1.1 (n = 8)
Grain size (μm)	0.10 ± 0.02 (n = 300)	0.10 ± 0.01 (n = 300)
Pore size (D50: μm)	0.07	0.06
Roughness (RA: μm)	14 ± 1 (n = 18)	7.1 ± 0.6 (n = 18)

[a]Value calculated from the chemical formula. Republished with permission of IOP Publishing, Ltd., from Osteoblast and osteoclast responses to A/B type carbonate-substituted hydroxyapatite ceramics for bone regeneration, Marie-Michèle Germaini, Rainer Detsch, Alina Grünewald, Amandine Magnaudeix, Fabrice Lalloué, Aldo R Boccaccini and Eric Champion, 12, 035008, 2017; permission conveyed through Copyright Clearance Center, Inc.

to that of the natural bone mineral on the other hand, i.e., carbonated HA with low crystallinity and highly reactive hydrated non-apatitic environments (Combes et al., 2016), an alternative to conventional high temperature sintering can be used by mean of flash sintering at very low temperature. The works from Ortali et al., succeeded in producing by this approach an amorphous carbonated calcium phosphate powder precipitated at the physiological temperature of 37°C. Spark plasma sintering at 150°C of this powder resulted in a consolidated ceramic made of calcium-deficient carbonated apatitic grains and hydrated non-apatitic grain boundaries. Hence, this new bioceramic mimicking bone chemistry is expected to have a higher bioreactivity than well crystallized carbonated hydroxyapatite ceramics (Ortali et al., 2018).

Effects of bioceramics micro-macroporous architecture on their colonization by cells and tissues

Scaffold architecture is of great importance for biological performances of a given osteoconductive material, especially regarding its colonization by host tissue when implanted. Architectural features were demonstrated to have influence on cell and tissue behavior at any scales, from nano to macro (Khang et al., 2012; Skoog et al., 2018; Jodati et al., 2020). Therefore, the scaffold architectural design constitutes a considerable strategy for improving bioceramics osteoconductivity even conferring osteoinductivity.

Bioceramic scaffolds may exhibit a multiscale porosity with a micro-porosity tuned by sintering parameters and a macroporosity (pore diameter >100 μm) lying on shaping. The micropores, obtained by incomplete sintering, have a typical diameter inferior to 10 μm and they are described as beneficial to the biological properties (Malmström et al., 2007; Zhang et al., 2014; Gariboldi and Best, 2015). Indeed, by increasing the exchange surface at the interface between the material and the biological milieu, the microporosity may enhance cell adhesiveness due to a better adsorption of the extracellular matrix adhesive proteins (Deligianni et al., 2000) and/or a better nutrient transfer (Malmström et al., 2007). These phenomena influence positively further cell activities such as osteogenic differentiation when considering osteoblast precursor cells. Microporosity-related increase of surface area also leads to a modification of the solubility of the material, altering back the release rate of chemical elements from calcium phosphate ceramics into the surrounding fluids (Gallo et al., 2018). The surface topography resulting from the presence of micropores is another factor that influences cell adhesion to the material surface (Rosa et al., 2003; Faia-Torres et al., 2014; Zhang et al., 2014). Microporosity is also of interest to serve as reservoir where bioceramics are intended to be functionalized and used as drug delivery systems (Arcos and Vallet-Regí, 2013).

Interconnected macropores (>100 μm) are intended to favour inner scaffold colonisation by new bone tissue and new blood vessels when the pore internal diameter is larger than 300 μm (Hutmacher et al., 2007). The geometry of the macropores in scaffolds influences the quality and the kinetics of their colonization by cell tissues (Rumpler et al., 2008; Knychala et al., 2013). This was mathematically modeled as the curvature-driven growth model and validated *in vitro* (Rumpler et al., 2008; Bidan et al., 2012; Bidan et al., 2013).

In two complementary works, we investigated the role of macropore geometry on their cell and tissue colonization using *in vitro* (Rüdrich et al., 2019) and *ex ovo* biological models (Magnaudeix et al., 2016). The *in vitro* study gave an overview of the way the cellular macropore colonization takes place (Rüdrich et al., 2019). The *ex ovo* model of chick chorioallantoic membrane (CAM) was a mean to evaluate the biomaterial vascularization (Magnaudeix et al., 2016). The CAM model is commonly employed to investigate the (anti) angiogenicity of compounds or the tumorigenicity and tumor angiogenesis (Ribatti et al., 2000; Ribatti, 2022).

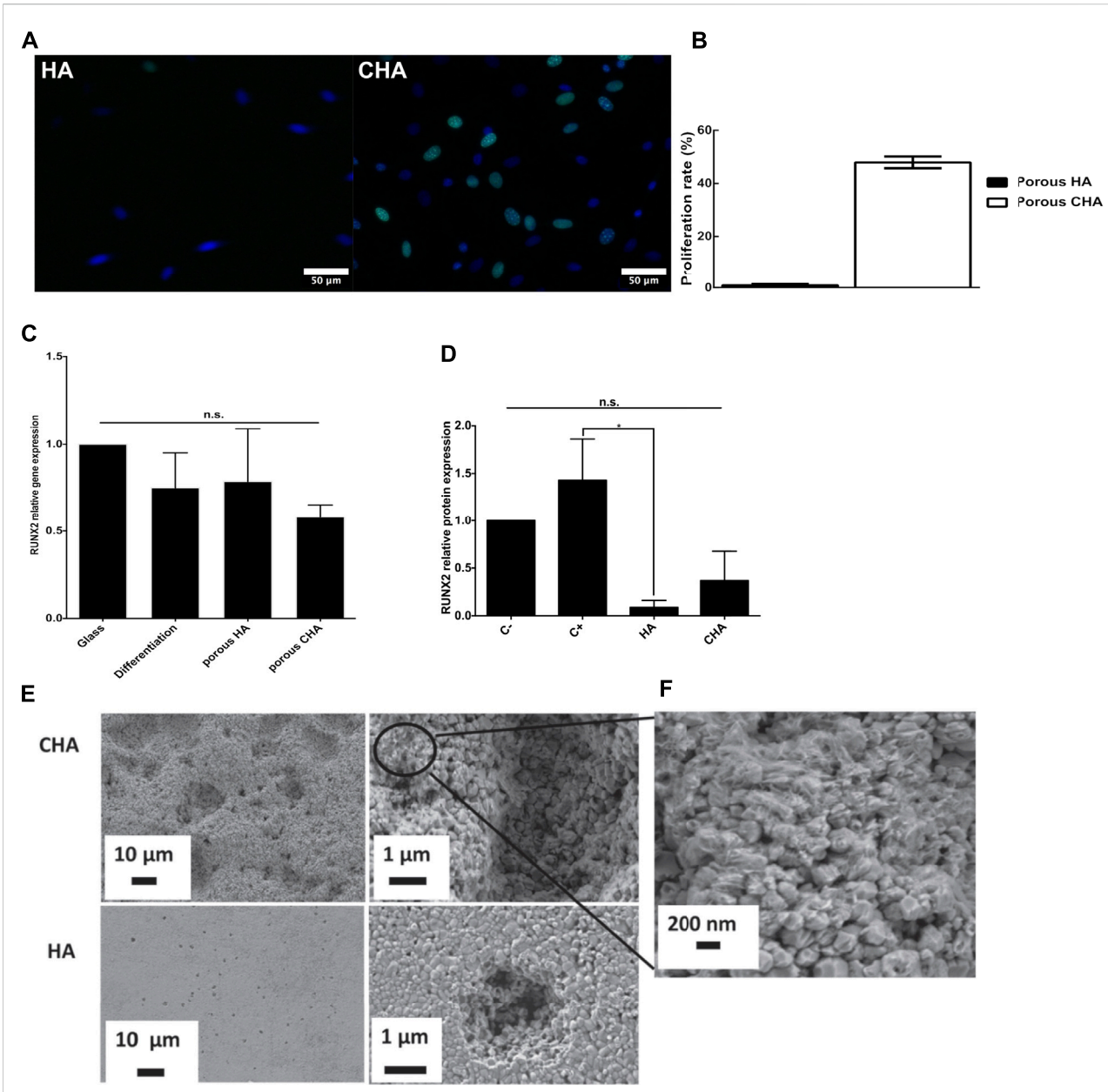

FIGURE 3
In vitro evaluation of carbonated hydroxyapatite bioceramics properties on MC3T3-E1 murine pre-osteoblasts and RAW264.7 cell line differentiation into osteoclast-like cells. **(A,B)** MC3T3-E1 pre-osteoblasts proliferation. **(A)** EdU assay microscopy images (green nuclei are EdU-positive and represent proliferating cells, nuclei, stained in blue by Hoechst 33342, feature total cells), scale bars: 100 µm. **(B)**Proliferation rate comparison (proliferating/total cells). Data are average values of ten analyzed areas on three independent pellets for each condition (total n = 30). **(C,D)** MC3T3-E1 pre-osteoblasts differentiation **(C).** Gene expression of RUNX2, after 7 days of culture, relativized with the internal control (glass coverslip). Positive controls correspond to cells cultured in a differentiation inductive culture medium. **(D)** Semi-quantitative analysis of RUNX2 protein expression analyzed in western-blotting. Actin was used as a loading control for MC3T3-E1 seeded directly on the pellet surface. n = 3. **(E,F)** Lacunae of resorption. **(E)** On HA and carbonated HA pellets after 14 days of RAW264.7 cell culture in osteoclastic differentiating medium. **(F)** Enlargement of carbonated HA pellets showing alteration of grain surface. Results are presented as means ± SD. Data were statistically analyzed using one-way ANOVA followed by a Fisher post-hoc test. n.s.: non significant $p < 0.05$: *,$p \leq 0.01$: ** and $p \leq 0.001$: ***. HA: hydroxyapatite, CHA: carbonated hydroxyapatite. Adapted with permission of IOP Publishing, Ltd., from Osteoblast and osteoclast responses to A/B type carbonate-substituted hydroxyapatite ceramics for bone regeneration, Marie-Michèle Germaini, Rainer Detsch, Alina Grünewald, Amandine Magnaudeix, Fabrice Lalloué, Aldo R Boccaccini and Eric Champion, 12, 035008, 2017; permission conveyed through Copyright Clearance Center, Inc.

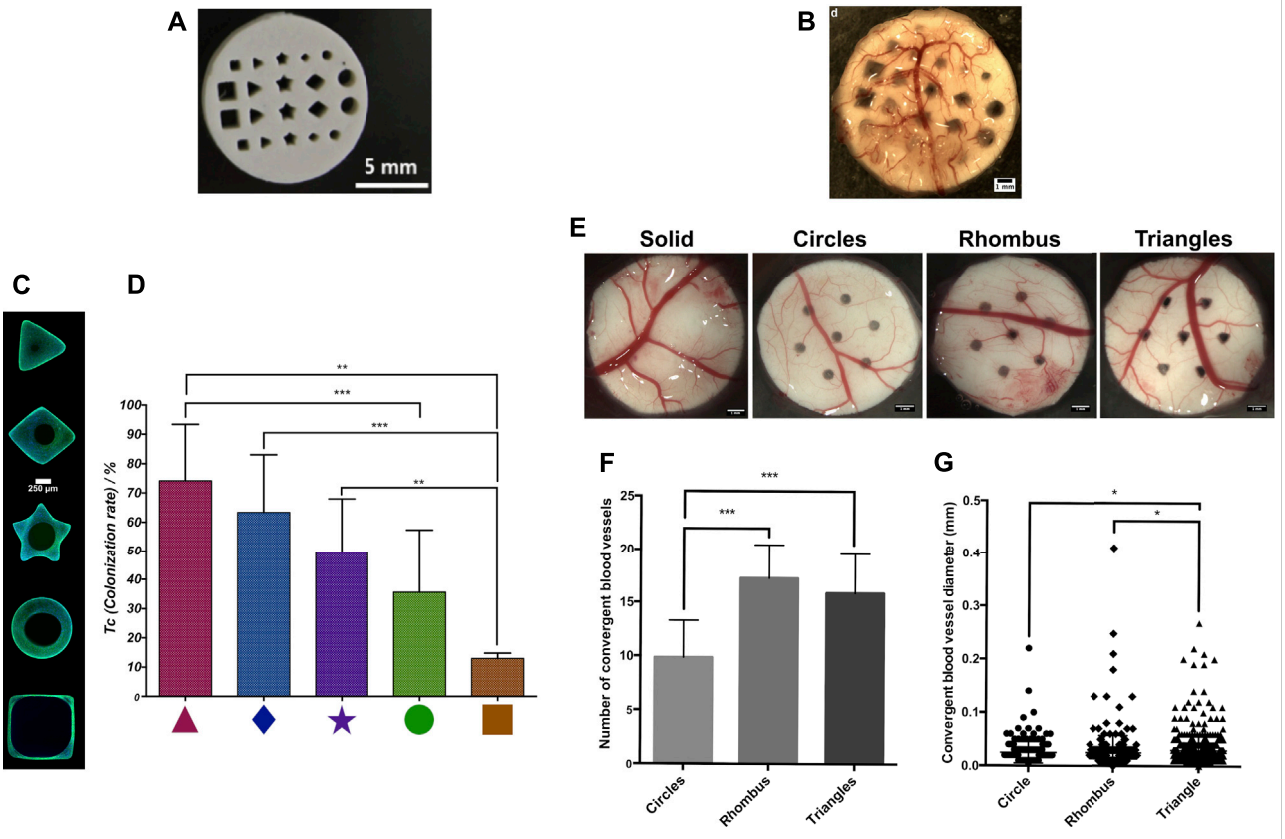

FIGURE 4
In vitro and *ex ovo* study of the influence of geometry of macropores on cell and tissue colonization. **(A)** View of a green sample of microporous silicon-substituted hydroxyapatite shaped by microstereolithography. **(B)** SiHA bioceramic with multi-shape pores after explantation from chick chorioallantoic membrane (CAM). **(C)** Microphotographs of colonized macropores by MC3T3-E1 pre-osteoblasts after 7 days of cell culture. Actin was stained with phalloidin conjugated to AlexaFluor488 (green), and nuclei were stained with Hoechst 33342 (blue). Scale bar: 250 µm **(D)**. Cellular colonization rates (Tcs) versus the macropore cross-section shape of dense silicon-substituted HA scaffolds. Statistics: two-way ANOVA followed by a Tukey's multiple comparison test. $p < 0.05$ was considered significant. *$p \leq 0.05$, **: $p \leq 0.01$; ***: $p \leq 0.001$. **(E)** Silicon susbstituted HA scaffolds featuring no pore or with a unique pore shape after explantation from CAM. Pictures were taken with a dissection microscope associated to a camera (magnification: ×16). **(F,G)** Analysis of blood vessels on silicon-substituted HA scaffolds featuring pores of a unique geometry. **(F)** Average number of blood vessels converging toward one pore of a defined geometry on a silicon substituted HA scaffold. **(G)** Diameter of blood vessels converging toward a pore in function of the pore shape. One-way ANOVA followed by a Tukey's multiple comparison test was used. $p < 0.05$ were considered as significant (*$p < 0.05$; **$p \leq 0.01$; ***$p \leq 0.001$). Adapted from Acta Biomaterialia, 38, Amandine Magnaudeix, Julie Usseglio, Marie Lasgorceix, Fabrice Lalloué, Chantal Damia, Joël Brie, Patricia Pascaud-Mathieu and Eric Champion, Quantitative analysis of vascular colonisation and angio-conduction in porous silicon-substituted hydroxyapatite with various pore shapes in a chick chorioallantoic membrane (CAM) model, Pages No. 179-189, and from Materials Science and Engineering: C, Urda Rüdrich, Marie Lasgorceix, Eric Champion, Patricia Pascaud-Mathieu, Chantal Damia, Joël Brie and Amandine Magnaudeix, Pre-osteoblast cell colonization of porous silicon substituted hydroxyapatite bioceramics: Influence of microporosity and macropore design, Pages No.510-528. Copyright (2022), with permission from Elsevier.

In both cases, we focused more especially on the influence of the 1) the presence and 2) the value of angles in the macropore geometry on the cell colonization behaviour inside the macropores. The co-influence of micropores into macropore walls was also evaluated (Rüdrich et al., 2019). The material composition was silicon-substituted hydroxyapatite (SiHA) (Palard et al., 2008). After SiHA powder synthesis, a photosensitive slurry was prepared to shape the scaffolds by an additive manufacturing technology, namely microstereolithography, with enough accuracy to allow a good definition of the macropores cross-sections at the pore size scale (Chartier et al., 2014; Lasgorceix et al., 2016). SiHA scaffolds were designed as ceramic disks containing transversal macropores varying in size, with a diameter of the equivalent circle comprised between 300 and 600 µm, and in their cross-sections geometries: circle, rhombus, triangle, star, and square (Figure 4A). To investigate the impact of additional microporosity on macropore colonization, an adjustment of the sintering parameters allowed to produce scaffolds having three different microstructures either dense (without open microporosity), with a medium open microporosity or highly microporous (open porosity amounts were 0,5 vol%, 23 vol% and

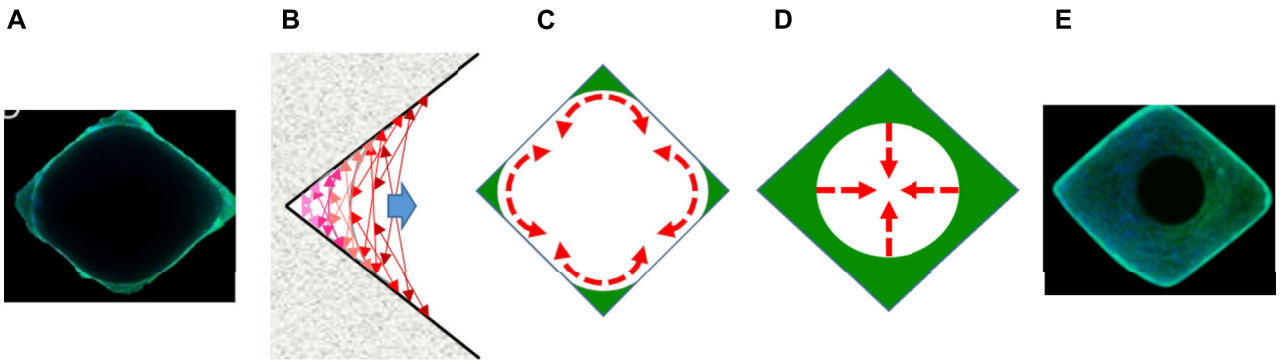

FIGURE 5
Schematic representation of the 2-step process of macropore colonization by cell tissue. **(A–C)** First step: cells progress along the pore wall until raise continuity. **(D,E)** Second step: cells progress towards the pore center. Here the pore geometry has no anymore influence. **(A,E)** Microphotographs of rhomboid macropores after 7 and 14 days of culture with MC3T3-E1 pre-osteoblasts. Actin was stained with phalloidin conjugated to AlexaFluor488 (green), and nuclei was stained with Hoechst 33342 (blue). **(C)** Representation of the curvature-driven model according to literature (Rumpler et al., 2008; Bidan et al., 2012, 2013). **(C,D)** schematic representation of cell progression in macropores.

27 vol% respectively). An increase of the surface area and a decrease of the grain size were obtained accordingly (Rüdrich et al., 2019).

The scaffolds were seeded with murine MC3T3-E1 pre-osteoblasts and cultured for 7–14 days (Figure 6) (Rüdrich et al., 2019) or implanted onto a chick chorioallantoic membrane for 4 days on 8.5 days old embryos (Figures 4B, E) (Magnaudeix et al., 2016). After having checked the biocompatibility of the SiHA bioceramics for both models, macropore colonization was first evaluated qualitatively, then quantitatively in order to rule out underlying mechanisms. Hence, we developed adapted computer-assisted image analysis methods based on the use of the NIH ImageJ software.[1] In the case of the cellular colonization, the use of multivariate statistical analysis methods (principal component analysis, PCA) helped to elucidate precisely which geometrical parameters could be involved in the cell colonization behaviour.

Macropore filling either by pre-osteoblasts or by developing vasculature

The main macroscopic results are presented in Figures 4, 6. In the *in vitro* model, as expected the filling rate was correlated to the size the macropores. In the absence of microporosity, we confirmed previous results from other works showing that the macropore colonization takes place in two-steps (Rumpler et al., 2008; Kommareddy et al., 2010; Bidan et al., 2012). In the first stage, the cells colonise the pore wall, up to their junction to form a cell tissue. During this step the influence of macropores geometry is maximal. After cell tissue formation, the cell colony progresses concentrically, in a centripetal way to fill the macropore, forming a circular hiatus until its closure which corresponds to the completion of the pore filling (Figure 5). When the colonization rate was examined according to the macropore cross-section geometry, it has been possible to establish significant differences and a classification of the macropore shape in function of their efficiency to be colonized from the triangles, the most colonized macropores, to the least ones the squares, rhombus, stars and circles being, respectively in the decreasing interval (Figures 6C,D). PCA analysis and a correlation matrix helped to identify determinant factors that were, first, the presence of acute angles as facilitating features of the geometry while re-entrant angles were deleterious. As convex surfaces (re-entrant angles), long flat surfaces of square sections were also lowly colonized. This overall tissue-like behavior is in accordance with the works of Nelson et al., on cellular growth in bulk tissues (Nelson et al., 2005). The acute/obtuse angle ratio appears then a relevant parameter to optimize the balance between flat lengths and concavities and explains the rather good colonization rate obtained in rhomboid macropores. This is consistent with the curvature-driven growth-model describing the importance of concavities for cells progression in macropores (Rumpler et al., 2008; Bidan et al., 2012; Bidan et al., 2013).

Similar results were observed at the tissue scale using the CAM model (Magnaudeix et al., 2016). The macroscopic examination of the blood vessel repartition has shown a preferential presence of blood vessels in the acute angles of the macropores containing these geometrical features. To go further, SiHA scaffolds with an unique geometry of macropores of same size were produced (Figure 4E). The angiogenesis, that

1 https://imagej.nih.gov/ij/.

corresponds to the formation of a new blood vessel from a pre-existing one, was not influenced by the presence of macropore neither by their geometry. But, at the whole SiHA ceramic implants scale, the analysis of blood vessel diameter in function of their hierarchy, i.e., if it is the parent vessel or a second or third order one, demonstrated that the presence of macropore by itself affected vascular guidance onto the surface of SiHA scaffolds. When the focus was straightened to the number and diameter of blood vessels converging toward macropores, two significant results were found. First, the number of converging blood vessels was greater when the macropores contained acute angles (i.e., triangle and rhombus vs. circle). Second, the average diameter of converging blood vessel was higher in triangular pores than rhomboid or circular ones. In other words, pores of cross-section geometry with acute angles (i.e., concavities at the microscopic level) were more attractive to guide the developing blood vessels than pores without angles (e.g., with a circular geometry) (Figures 4F,G).

In summary, different and complementary biological models responded in a similar way to similar cues. The first model (*in vitro* culture of pre-osteoblastic cells) corresponded to individual cells with a tissue like organization and the other one to a well-organized tissue made of different cell types and their associated extracellular matrix (*ex ovo* CAM model). Interestingly, the extent of the influence of macropore geometries appeared higher in the case of the tissue model in comparison with the cellular model: blood vessels were mainly located in sharp angles and very few or none were found in re-entrant angles. Consequently, one can emit the hypothesis that here, strong cell-cell interactions involving cytoskeleton, and at a higher level cell communication through local release of growth factors (such as VEGF as a driving force in the context of angiogenesis) may create a synergistic influence with scaffold positive cues for cell guidance.

Microporosity addition impedes the influence of macropore geometries on cell colonization

Results from *in vitro* macropore colonization assays using microporous SiHA scaffolds demonstrated that the additional presence of open microporosity interfered negatively with macropore geometrical effects on cell in-growth (Figure 6A) (Rüdrich et al., 2019). In this latter case, whatever the macropore geometries might be, the colonization rate was directly inversely correlated to the amount of open porosity in the scaffolds while the cell growth on plain surfaces was not affected (Figure 6B). Moreover, the influence of cross-section geometries on macropore filling by cell was lost (Figure 6C). Even the direct inverse correlation between pore size and colonization rate disappeared. Interestingly, visually, the circularity of the hiatus formed by the cell filling concentrically the macropores was altered in the presence of open microporosity. Since no modification of cell growth was evidenced on plane surfaces, we hypothesized that the negative impact of microporosity is likely due to a modification of bioceramics surface topography and takes place very early during the pore colonization process during the adhesion step of the cell at the surface of macropore walls. As described earlier, a layered organization of the cells was detected on dense walls, whereas it was not easy to perceive in the presence and increase of open microporosity amount (Figure 6D). In an advanced model of the curvature-driven growth called "chord model" (Figure 6E) including the cell scale level, Bidan et al., have proposed that the surface topography between the adhesion points of a cell influences its spreading on concave surfaces. Thus, the cells fit the surface by stretching their membranes, while they stay curved and exert pressure on convex surfaces of the substrate (Bidan et al., 2012). In other words, after having adhered to a surface, cells contract their cytoskeleton to acquire a stable tension state, consuming less energy. Therefore, the presence of acute angles assimilated to surface concavities/curvatures facilitated the cell tissue progression through mechano-biological processes based on actin cytoskeleton modifications. But, the modification of surface properties (topography, roughness) due to the microstructure may alter the way cells adhere to the material and to each other, affecting the cell cytoskeleton organization. This structure is of high importance for the establishment of cell-cell contacts, junctions and other interactions. Hence, we can hypothesize that by altering tissue-like organization of the cells, the presence of microporosity slows down their progression during pore colonization.

The information collected can help to understand and develop optimised microporous scaffold even if in 3D dynamic conditions supplementary physical cues can modulate the phenomena observed in 2D static conditions. Another interesting point is that biological models at two different scales react similarly while it is proven that different cell types do not react in the same way to the chemical-physical properties of their microenvironment. The importance to consider cell-cell communication and the tissue scale when evaluating the biological properties of ceramic materials is now recognized. This also raises the need of more accurate *in vitro* models for evaluating the biological performances of bone substitutes taking account the tridimensionality of the living (discussed in (Champion et al., 2017)). Finally, the multivariate statistical approach can be adopted for a more comprehensive biological evaluation of bioceramics where each change made during the elaboration process induces multiple modifications at the chemical physical level and by extension changes of the biological response. Such an approach would also help to bring out a better reproducibility and comparability between the available results of the abundant researches on ceramics and other materials for bone tissue engineering.

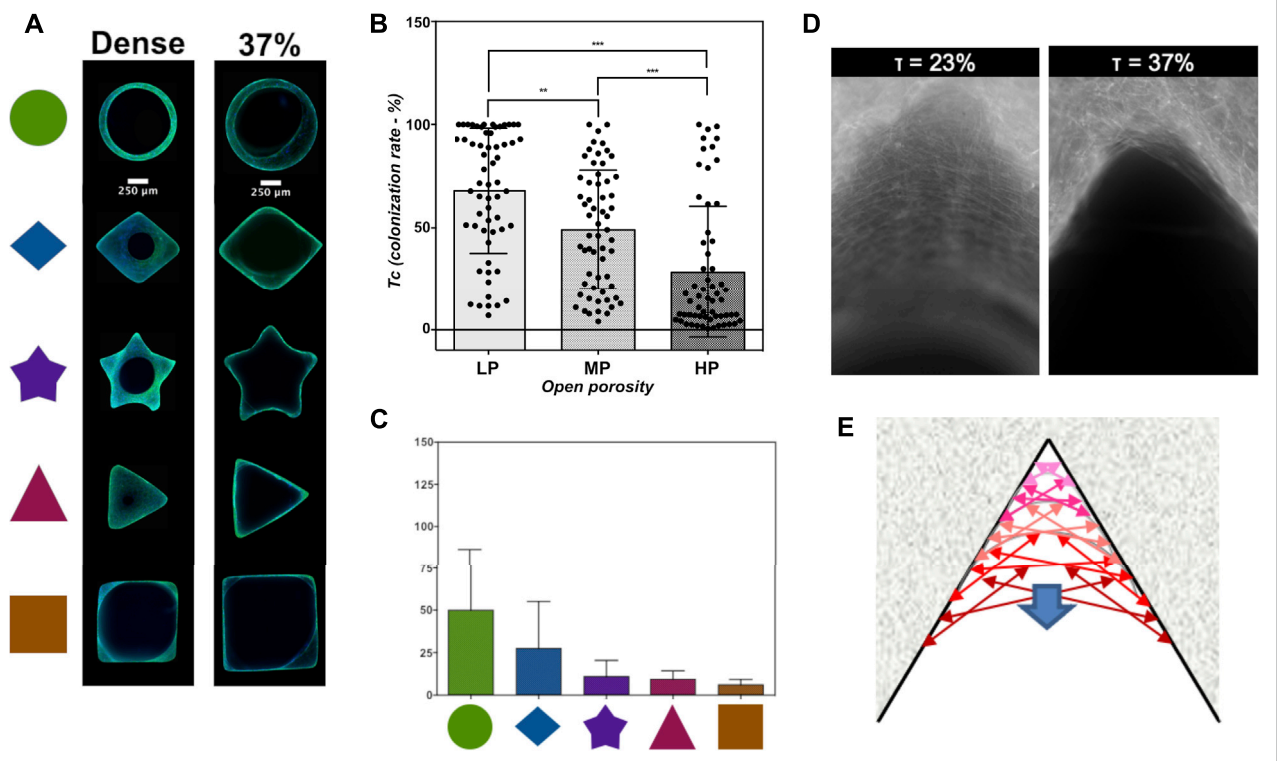

FIGURE 6
Influence of microporosity in macropore walls on their cellular colonization. **(A)** Microphotographs of colonized macropores by MC3T3-E1 pre-osteoblasts after 7 days of cell culture. Actin was stained with phalloidin conjugated to AlexaFluor488 (green), and nuclei were stained with Hoechst 33342 (blue). Scale bar: 250 µm. **(B)** Effect of open microporosity on average colonization rate of macropores (Tc) ± S.D. Statistics: Kruskall-Wallis test followed by a Dunn's multiple comparison test. $p < 0.05$ was considered significant. **: $p \leq 0.01$; ***: $p \leq 0.001$. **(C)** Cellular colonization rates (Tcs) versus the macropore cross-section shape of silicon-substituted HA scaffolds with an open microporosity rate of 37 vol%. Statistics: two-way ANOVA followed by a Tukey's multiple comparison test. $p < 0.05$ was considered significant. *$p \leq 0.05$, **: $p \leq 0.01$; ***: $p \leq 0.001$. **(D).** Microphotographs of the actin cytoskeleton of MC3T3-E1 pre-osteoblasts having colonized acute angles on triangular macropore of dense (open microporosity rate: 0.5 vol%) or microporous (open microporosity rate: 37 vol%) of silicon-substituted scaffolds. **(E)** Representation of the curvature-driven model according to literature (Rumpler et al., 2008; Bidan et al., 2012; Bidan et al., 2013). Some parts of the figure are adapted from Materials Science and Engineering: C, Urda Rüdrich, Marie Lasgorceix, Eric Champion, Patricia Pascaud-Mathieu, Chantal Damia, Joël Brie and Amandine Magnaudeix, Pre-osteoblast cell colonization of porous silicon substituted hydroxyapatite bioceramics: Influence of microporosity and macropore design, Pages No. 510-528. Copyright (2022), with permission from Elsevier.

Functionalization

Once ceramic scaffolds are produced, a last major lever for enhancing their applicative performances is to functionalize their surface with molecules able to confer them superior biological properties (Hench and Polak, 2002). The new targeted functions can directly relate to the properties required for a biomaterial to meet or at least to get closer to the ideal bone substitute as defined above. The new functions can also target a complementary therapeutic treatment. In this scope, HA-bioceramics have been extensively used to develop drug delivery systems for various medical applications that are, in the case of calcium-phosphate bioceramics, mostly related to the bone tissue (Arcos and Vallet-Regí, 2013). Amongst them: struggle against post-operative infections that constitutes a major public health issue (Simchi et al., 2011; Walter et al., 2021), anti-tumoral therapies targeting bone cancer (Bischoff et al., 2018), limitation of inflammation (Lasgorceix et al., 2014), etc. Logically, the nature of molecule associated to the bioceramics surface depends of the targeted applications: antibiotics, anti-inflammatory molecules or chemotherapeutic agents are employed (Lasgorceix et al., 2014; Parent et al., 2016; Bischoff et al., 2018). The functionalization of biomaterials used as bone substitutes by antibiotics is developed to counter the drawbacks of systemic administration of high doses of antibiotics to treat post-operative bone infections. A local delivery of lower doses of the substance than those taken by classical oral or parenteral administration is expected to have high efficiency, minimize the development of bacterial resistances or of other side effects. Such antibiotic-loaded biomaterials are intended to prevent infection in a prophylactic strategy despite mixed results (Masters et al., 2022). Alternatively, a strategy of functionalization of

biomaterials with bacteriophages that are viruses with a bactericide action is also developed (Rotman et al., 2020).

The molecules of interest can be immobilized at the ceramic surface by two methods: physical or chemical absorption or covalent chemical bonding (Parent et al., 2016; Damia et al., 2021). HA have a great ability to adsorb biomolecules at its surface. Microporous bioceramics are materials of choice in this context. By increasing the specific surface area, the microporosities provide a drug reservoir allowing a better loading of the functionalizing molecule (Baradari et al., 2012). In this case it is important to understand the interactions between the bioceramic and the molecule in order to control and optimize both, its loading and release (Parent et al., 2016). But it is also of prime importance to evaluate the consequences on bone healing. With this aim, we loaded microporous HA bioceramics with vancomycin (Parent et al., 2016). Vancomycin is a broad-spectrum antibiotic with a low-frequency resistance that can be used against *Staphylococcus aureus*. *S. aureus* is the pathogen responsible for a majority of post-operative bone infections is *S. aureus* (Wassif et al., 2021). This gram-positive bacteria is often resistant to a variety of antiobiotics and vancomycin was an obvious choice in this context (Urish and Cassat, 2020). In a first experimental set, we have shown that the antibiotic was non linearly loaded at the surface of the material with a fast uptake for 15 min followed by a slowing down of the adsorption kinetics. Interestingly, depending of the concentration of the vancomycin solution used for HA loading, the release kinetics of the antibiotic in a biological medium differed. With the highest tested concentration, i.e., 50 mg/ml, a complete release was achieved in 5 days, against 24 h for lower doses. All the vancomycin-loaded materials presented a bacteriostatic and a bactericidal activity. But, the device must not only be efficient in meeting this need, a key point is that its biological properties must remain satisfying. To make sure of it, we have tested the biocompatibility of these materials towards bone cells. An impairment of pre-osteoblast adhesion to the material surface was evidenced in the early steps after seeding. A slowdown of cell migration at the ceramic surface was observed with the highest dose of loaded vancomycin. However, cell proliferation was not affected (Parent et al., 2016).

Physiologically, the bone repair implies the sequential and coordinated involvement in the time of cellular actors from immune, vascular and skeletal system in the time. In a biomimetic approach, the ideal material will induce events allowing this enchainment of processes to take place (Lopes et al., 2018). Biomaterial functionalization can be a useful tool for this purpose. The stimulation of specific cell activities can be achieved by proteins or derived peptides with adhesive functions (e.g., extracellular matrix adhesive protein or the related amino acid motifs recapitulating their function) or with stimulatory/regulatory activities (e.g., growth factors, ECM small regulatory proteins or cytokines) (Lopes et al., 2018; Damia et al., 2021). In the case of adhesive proteins or short peptides, the strategy can be to adsorb them (Schneiders et al., 2007; Hennessy et al., 2008) or to covalently graft them (Durrieu et al., 2004) on the biomaterial surface. In this regard, we successfully functionalized silicon-substituted hydroxyapatite ceramics with an adhesive peptide. This peptide was a cyclic pentapeptide, c-(DfKRG) containing the minimal amino-acid sequence presenting a biological activity, namely the RGD peptide, identified in the fibronectin ECM protein (Pierschbacher and Ruoslahti, 1984; Hynes, 2009). The major drawback of the adsorption process remains the biomolecule delivery (kinetics and actually released amounts) which is usually poorly controlled. We developed an advanced 2-step protocol to covalently bond the molecule of interest to the material surface. This method allowed us to control the binding density while limiting contamination by adsorbed byproducts due to the successive *in situ* steps used for achieving the covalent binding (Poli et al., 2019). First, an organosilane, 3-aminopropyltriethoxysilane (APTES), was covalently bounded onto the surface of the bioceramic. Then, the peptide, bearing a spacer molecule, PEG_6, in order to preserve its conformation and to make it easily available for the cells was covalently attached to the APTES by a click-chemistry reaction. After having characterized and evaluated the efficiency of the covalent binding of the c(DfKRG), we characterized its functionality, i.e., we evaluated, at several time-points, if the functionalized bioceramic stimulated adhesion and/or proliferation of bone cells at the surface of the biomaterial in comparison with a non-functionalized one. The robustness of the covalent bond was also evaluated by re-using the functionalized SiHA bioceramics after cleaning-sterilization cycles. At each step, the biocompatibility of the SiHA was not affected by the functionalization. Two successful consecutive reuses proved the preservation of both the structural integrity and the biological activity of the immobilized peptide since cell density adhesion, and cell proliferation were enhanced (Poli et al., 2019).

Adsorption and covalent bonding are also the common routes employed to functionalize bioceramics with recombinant full length growth factors (Hajimiri et al., 2015; Damia et al., 2021). The main growth factors chosen to functionalize bioceramics for application in bone repair are the osteogenic bone morphogenetic protein-2 (BMP-2) and the vascular endothelial growth factor VEGF (Aryal et al., 2014; Damia et al., 2021), alone (Damia et al., 2019; Casarrubios et al., 2020) or in combination together (Kanczler et al., 2010; Schorn et al., 2017) or with other growth factors (Ratanavaraporn et al., 2011; Shen et al., 2016; Kuhn et al., 2021). BMP-2 and VEGF, as signaling molecules, play central roles in the molecular events controlling the spatial-temporal accomplishment of bone healing (Salhotra et al., 2020). BMP-2, is the key growth factor for osteogenesis and is used in clinical practice (El Bialy et al., 2017; Lowery and Rosen, 2018) especially for spine fusion because of its potent osteogenic effect. However, likely due to an administration at supraphysiological doses, severe adverse effects were reported (James et al., 2016;

Kowalczewski and Saul, 2018). These concerns relate to an uncontrolled release, in terms of dose and kinetics, which currently limits the clinical use of recombinant human BMP-2 (rhBMP-2) (El Bialy et al., 2017). The high potency of VEGF and its implication in several pathological molecular mechanisms such as age-related macular degeneration in its neovascular form (Thomas et al., 2021) or tumoral angiogenesis (for which molecules targeted the VEGF are therapeutical approaches) may raise the same concerns as BMP-2, taken as an example here.

In this context the covalent bonding of growth factors to the biomaterial surface is a seducing approach, alternative to absorption, which is associated to a weak bond that does not allow control release of the molecule (Damia et al., 2019). In the work from (Damia et al., 2019), rhBMP-2 was covalently attached to silicated hydroxyapatite microspheres by silanization with APTES. A PEG_6 spacer attached to the silane to allowed to maintain a minimal distance for a proper function of the attached protein. Then, rhBMP-2 was attached to the system thanks to the previous addition of a NHS group to rhBMP-2, using the same click-chemistry reaction as in (Poli et al., 2019). Interestingly, in this setting, the chemical characterization have demonstrated that rhBMP-2 was grafted at a low density on the ceramic surface (around 4.10^{-8} $mol.g^{-1}$). A modified C3H10 sarcoma cell line that express the firefly luciferase reporter gene under the control of BRE (bone morphogenetic protein (BMP) responsive element) was used to evaluate the bioactivity of the immobilized rhBMP-2. The luciferase expression evidenced a successful signal transduction linked to the binding of rhBMP-2 to its receptor at the cell surface. A significant expression of luciferase was detected when the cells were cultured in the presence of the SiHA microspheres bearing rhBMP-2 demonstrating that rhBMP-2 has retained its activity. The expression of luciferase was equivalent in intensity to those of cells stimulated with soluble BMP-2 around 10–30 ng/ml. Such a dosage was shown to be sufficient to induce bone repair in dog with no adverse effect (Gibbs et al., 2016). This approach, that also allows to increase significantly the growth factor half-life (Schickle et al., 2011; Damia et al., 2019) should be completed by the use of cleavable spacers in order to better control the release with time. Spacers cleavable in different ways should allow to immobilize different and complementary growth factor for a sequential and controlled release with time that may fit with the physiological molecular mechanism of action of BMP-2, which is an important point to consider as highlighted by (Kowalczewski and Saul, 2018).

Therefore, biocompatibility and bioactivity assessment are once again essential not only to validate the material functionality but also to rationalize and optimize its develop.

Applications in the clinical practice

Calcium phosphate ceramics are used for clinical applications since the 1980's. More recently, ceramic scaffolds of personalized architectures produced by additive manufacturing have been available for bone repair, e.g., Custombone™ (Amelot et al., 2021).

Amongst the different strategies to enhance bioceramics biological properties that are exemplified throughout this paper, doping of calcium phosphate ceramics, while an extensive worldwide research, is not yet really effective in clinic. This observation was already made a few years ago by M. Šupová in a review paper (Šupová, 2015) and it is still valuable. Nevertheless, some micro-macro-porous silicon substituted calcium phosphate scaffolds are available: Actifuse™ (Lerner and Liljenqvist, 2013; Szurkowska and Kolmas, 2017) and Inductigraft™ (Bolger et al., 2019), that differ by their porosity amount with application in spine surgery.

Finally, combination of active molecules to biomaterials is used in the context of infection treatment. For example porous alumina sternal implants loaded with antibiotics are successfully used to treat severe bone infections (Bertin et al., 2018; Tricard et al., 2020). As discussed above rhBMP-2 is approved for medical applications but restricted mainly in spinal surgery under soluble form (El Bialy et al., 2017; Kowalczewski and Saul, 2018).

Concluding remarks

The "ideal" material is a compromise of features acting positively on most of these cellular events associated to bone regeneration (Lopes et al., 2018). Their complexity also likely explains discrepancies concerning results regarding biological properties of given biomaterials. Consequently, there is a true need for a reliable characterization of biological features of the calcium phosphate ceramics for bone tissue engineering discriminating the impact of the material chemical and physical properties. To understand how the chemical-physical properties of the material impact cell behavior according to the cell type will allow to rationalize the research in this field. This imply, that this enthusiastic research about biomaterials for bone tissue engineering is necessarily multi and transdisciplinary.

Author contributions

AM drafted, wrote and edited the manuscript and designed the original figures.

Funding

This work and most of our works cited in this manuscript were funded by institutional grants from the French Research National Agency (ANR—Agence Nationale de la Recherche): project CharaBioC (ANR-19-CE08-0003-01) and LabEX SigmaLim (ANR-10-LABX-0074-01).

Acknowledgments

The author would like to thanks Prof. E. Champion for proofreading of the manuscript and all the persons of our team who have contributed to our works presented here.

Conflict of interest

The author declares that the research was conducted in the absence of any commercial or financial relationships that could be construed as a potential conflict of interest.

Publisher's note

All claims expressed in this article are solely those of the authors and do not necessarily represent those of their affiliated organizations, or those of the publisher, the editors and the reviewers. Any product that may be evaluated in this article, or claim that may be made by its manufacturer, is not guaranteed or endorsed by the publisher.

References

Amelot, A., Nataloni, A., François, P., Cook, A.-R., Lejeune, J.-P., Baroncini, M., et al. (2021). Security and reliability of custombone cranioplasties: A prospective multicentric study. *Neurochirurgie* 67, 301–309. doi:10.1016/j.neuchi.2021.02.007

Arcos, D., and Vallet-Regí, M. (2013). Bioceramics for drug delivery. *Acta Mater.* 61, 890–911. doi:10.1016/j.actamat.2012.10.039

Aryal, R., Chen, X., Fang, C., and Hu, Y. (2014). Bone morphogenetic protein-2 and vascular endothelial growth factor in bone tissue regeneration: New insight and perspectives: BMP-2 & VEGF in bone tissue regeneration. *Orthop. Surg.* 6, 171–178. doi:10.1111/os.12112

Baradari, H., Damia, C., Dutreih-Colas, M., Laborde, E., Pécout, N., Champion, E., et al. (2012). Calcium phosphate porous pellets as drug delivery systems: Effect of drug carrier composition on drug loading and *in vitro* release. *J. Eur. Ceram. Soc.* 32, 2679–2690. doi:10.1016/j.jeurceramsoc.2012.01.018

Bazin, T., Magnaudeix, A., Mayet, R., Carles, P., Julien, I., Demourgues, A., et al. (2021). Sintering and biocompatibility of copper-doped hydroxyapatite bioceramics. *Ceram. Int.* 47, 13644–13654. doi:10.1016/j.ceramint.2021.01.225

Bernhardt, A., Bacova, J., Gbureck, U., and Gelinsky, M. (2021). Influence of Cu2+ on osteoclast formation and activity *In vitro*. *Int. J. Mol. Sci.* 22, 2451. doi:10.3390/ijms22052451

Bertin, F., Piccardo, A., Denes, E., Delepine, G., and Tricard, J. (2018). Porous alumina ceramic sternum: A reliable option for sternal replacement. *Ann. Thorac. Med.* 13, 226. doi:10.4103/atm.ATM_80_18

Bidan, C. M., Kommareddy, K. P., Rumpler, M., Kollmannsberger, P., Bréchet, Y. J. M., Fratzl, P., et al. (2012). How linear tension converts to curvature: Geometric control of bone tissue growth. *PLoS ONE* 7, e36336. doi:10.1371/journal.pone.0036336

Bidan, C. M., Kommareddy, K. P., Rumpler, M., Kollmannsberger, P., Fratzl, P., and Dunlop, J. W. C. (2013). Geometry as a factor for tissue growth: Towards shape optimization of tissue engineering scaffolds. *Adv. Healthc. Mater.* 2, 186–194. doi:10.1002/adhm.201200159

Bischoff, I., Tsaryk, R., Chai, F., Fürst, R., Kirkpatrick, C. J., and Unger, R. E. (2018). *In vitro* evaluation of a biomaterial-based anticancer drug delivery system as an alternative to conventional post-surgery bone cancer treatment. *Mater. Sci. Eng. C* 93, 115–124. doi:10.1016/j.msec.2018.07.057

Bolger, C., Jones, D., and Czop, S. (2019). Evaluation of an increased strut porosity silicate-substituted calcium phosphate, SiCaP EP, as a synthetic bone graft substitute in spinal fusion surgery: A prospective, open-label study. *Eur. Spine J.* 28, 1733–1742. doi:10.1007/s00586-019-05926-1

Bose, S., Fielding, G., Tarafder, S., and Bandyopadhyay, A. (2013). Understanding of dopant-induced osteogenesis and angiogenesis in calcium phosphate ceramics. *Trends Biotechnol.* 31, 594–605. doi:10.1016/j.tibtech.2013.06.005

Brie, J., Chartier, T., Chaput, C., Delage, C., Pradeau, B., Caire, F., et al. (2013). A new custom made bioceramic implant for the repair of large and complex craniofacial bone defects. *J. Cranio-Maxillofacial Surg.* 41, 403–407. doi:10.1016/j.jcms.2012.11.005

Brunel, A., Pagès, E., Magnaudeix, A., and Champion, É. (2021). "Influence of copper-substitution in calcium phosphate ceramics on endothelial cells," in 31st Conference of the European Society for Biomaterials, Porto, October 5–9, 2021 (online), Poster.

Brydone, A. S., Meek, D., and Maclaine, S. (2010). Bone grafting, orthopaedic biomaterials, and the clinical need for bone engineering. *Proc. Inst. Mech. Eng. H.* 224, 1329–1343. doi:10.1243/09544119JEIM770

Burghardt, I., Lüthen, F., Prinz, C., Kreikemeyer, B., Zietz, C., Neumann, H.-G., et al. (2015). A dual function of copper in designing regenerative implants. *Biomaterials* 44, 36–44. doi:10.1016/j.biomaterials.2014.12.022

Calori, G. M., and Giannoudis, P. V. (2011). Enhancement of fracture healing with the diamond concept: the role of the biological chamber. *Injury* 42, 1191–1193. doi:10.1016/j.injury.2011.04.016

Casarrubios, L., Gómez-Cerezo, N., Sánchez-Salcedo, S., Feito, M. J., Serrano, M. C., Saiz-Pardo, M., et al. (2020). Silicon substituted hydroxyapatite/VEGF scaffolds stimulate bone regeneration in osteoporotic sheep. *Acta Biomater.* 101, 544–553. doi:10.1016/j.actbio.2019.10.033

Champion, E., Magnaudeix, A., Pascaud-Mathieu, P., and Chartier, T. (2017). "Advanced processing techniques for customized ceramic medical devices," in *Advances in ceramic biomaterials* (Elsevier), 433–468. doi:10.1016/B978-0-08-100881-2.00015-4

Champion, E. (2013). Sintering of calcium phosphate bioceramics. *Acta Biomater.* 9, 5855–5875. doi:10.1016/j.actbio.2012.11.029

Charbonnier, B., Hadida, M., and Marchat, D. (2021). Additive manufacturing pertaining to bone: Hopes, reality and future challenges for clinical applications. *Acta Biomater.* 121, 1–28. doi:10.1016/j.actbio.2020.11.039

Chartier, T., Dupas, C., Lasgorceix, M., Brie, J., Delhote, N., and Chaput, C. D. (2014). Additive manufacturing to produce complex 3D ceramic parts. *J. Ceram. Sci. Technol.* 6, 95–104. doi:10.4416/JCST2014-00040

Combes, C., Cazalbou, S., and Rey, C. (2016). Apatite biominerals. *Minerals* 6, 34. doi:10.3390/min6020034

Costa, D. O., Prowse, P. D. H., Chrones, T., Sims, S. M., Hamilton, D. W., Rizkalla, A. S., et al. (2013). The differential regulation of osteoblast and osteoclast activity by surface topography of hydroxyapatite coatings. *Biomaterials* 34, 7215–7226. doi:10.1016/j.biomaterials.2013.06.014

Damia, C., Magnaudeix, A., and Laverdet, B. (2021). "Chemical functionalization of calcium phosphate bioceramic surfaces," in *Encyclopedia of materials: Technical ceramics and glasses*. Editor M. Pomeroy (Oxford: Elsevier), 716–731. doi:10.1016/B978-0-12-803581-8.12108-3

Damia, C., Marchat, D., Lemoine, C., Douard, N., Chaleix, V., Sol, V., et al. (2019). Functionalization of phosphocalcic bioceramics for bone repair applications. *Mater. Sci. Eng. C* 95, 343–354. doi:10.1016/j.msec.2018.01.008

Deligianni, D. D., Katsala, N. D., Koutsoukos, P. G., and Missirlis, Y. F. (2000). Effect of surface roughness of hydroxyapatite on human bone marrow cell adhesion, proliferation, differentiation and detachment strength. *Biomaterials* 22, 87–96. doi:10.1016/S0142-9612(00)00174-5

Durrieu, M. C., Pallu, S., Guillemot, F., Bareille, R., Amédée, J., Baquey, C., et al. (2004). Grafting RGD containing peptides onto hydroxyapatite to promote osteoblastic cells adhesion. *J. Mater. Sci. Mater. Med.* 15, 779–786. doi:10.1023/B:JMSM.0000032818.09569.d9

El Bialy, I., Jiskoot, W., and Reza Nejadnik, M. (2017). Formulation, delivery and stability of bone morphogenetic proteins for effective bone regeneration. *Pharm. Res.* 34, 1152–1170. doi:10.1007/s11095-017-2147-x

Elliott, J. C. (1994). *Structure and chemistry of the apatites and other calcium orthophosphates*. Amsterdam: Elsevier Science. Available at: http://qut.eblib.com.au/patron/FullRecord.aspx?p=1837764 (Accessed July 1, 2022).

Faia-Torres, A. B., Guimond-Lischer, S., Rottmar, M., Charnley, M., Goren, T., Maniura-Weber, K., et al. (2014). Differential regulation of osteogenic differentiation of stem cells on surface roughness gradients. *Biomaterials* 35, 9023–9032. doi:10.1016/j.biomaterials.2014.07.015

Gallo, M., Tadier, S., Meille, S., and Chevalier, J. (2018). Resorption of calcium phosphate materials: Considerations on the *in vitro* evaluation. *J. Eur. Ceram. Soc.* 38, 899–914. doi:10.1016/j.jeurceramsoc.2017.07.004

Gariboldi, M. I., and Best, S. M. (2015). Effect of ceramic scaffold architectural parameters on biological response. *Front. Bioeng. Biotechnol.* 3, 151. doi:10.3389/fbioe.2015.00151

Germaini, M.-M., Detsch, R., Grünewald, A., Magnaudeix, A., Lalloue, F., Boccaccini, A. R., et al. (2017). Osteoblast and osteoclast responses to A/B type carbonate-substituted hydroxyapatite ceramics for bone regeneration. *Biomed. Mat.* 12, 035008. doi:10.1088/1748-605X/aa69c3

Giannoudis, P. V., Einhorn, T. A., and Marsh, D. (2007). Fracture healing: The diamond concept. *Injury* 38, S3–S6. S3–S6. doi:10.1016/S0020-1383(08)70003-2

Gibbs, D. M. R., Black, C. R. M., Hulsart-Billstrom, G., Shi, P., Scarpa, E., Oreffo, R. O. C., et al. (2016). Bone induction at physiological doses of BMP through localization by clay nanoparticle gels. *Biomaterials* 99, 16–23. doi:10.1016/j.biomaterials.2016.05.010

Gomes, S., Vichery, C., Descamps, S., Martinez, H., Kaur, A., Jacobs, A., et al. (2018). Cu-doping of calcium phosphate bioceramics: From mechanism to the control of cytotoxicity. *Acta Biomater.* 65, 462–474. doi:10.1016/j.actbio.2017.10.028

Hajimiri, M., Shahverdi, S., Kamalinia, G., and Dinarvand, R. (2015). Growth factor conjugation: Strategies and applications: Growth factor conjugation. *J. Biomed. Mat. Res.* 103, 819–838. doi:10.1002/jbm.a.35193

Hench, L. L., and Polak, J. M. (2002). Third-generation biomedical materials. *Science* 295, 1014–1017. doi:10.1126/science.1067404

Hennessy, K. M., Clem, W. C., Phipps, M. C., Sawyer, A. A., Shaikh, F. M., and Bellis, S. L. (2008). The effect of RGD peptides on osseointegration of hydroxyapatite biomaterials. *Biomaterials* 29, 3075–3083. doi:10.1016/j.biomaterials.2008.04.014

Ho-Shui-Ling, A., Bolander, J., Rustom, L. E., Johnson, A. W., Luyten, F. P., and Picart, C. (2018). Bone regeneration strategies: Engineered scaffolds, bioactive molecules and stem cells current stage and future perspectives. *Biomaterials* 180, 143–162. doi:10.1016/j.biomaterials.2018.07.017

Hui, Y., Dong, Z., Wenkun, P., Yao, D., Huichang, G., and Tongxiang, L. (2020). Facile synthesis of copper doping hierarchical hollow porous hydroxyapatite beads by rapid gelling strategy. *Mater. Sci. Eng. C* 109, 110531. doi:10.1016/j.msec.2019.110531

Hutmacher, D. W., Schantz, J. T., Lam, C. X. F., Tan, K. C., and Lim, T. C. (2007). State of the art and future directions of scaffold-based bone engineering from a biomaterials perspective. *J. Tissue Eng. Regen. Med.* 1, 245–260. doi:10.1002/term.24

Hynes, R. O. (2009). The extracellular matrix: Not just pretty fibrils. *Science* 326, 1216–1219. doi:10.1126/science.1176009

James, A. W., LaChaud, G., Shen, J., Asatrian, G., Nguyen, V., Zhang, X., et al. (2016). A review of the clinical side effects of bone morphogenetic protein-2. *Tissue Eng. Part B Rev.* 22, 284–297. doi:10.1089/ten.teb.2015.0357

Jodati, H., Yılmaz, B., and Evis, Z. (2020). A review of bioceramic porous scaffolds for hard tissue applications: Effects of structural features. *Ceram. Int.* 46, 15725–15739. doi:10.1016/j.ceramint.2020.03.192

Kanczler, J. M., Ginty, P. J., White, L., Clarke, N. M. P., Howdle, S. M., Shakesheff, K. M., et al. (2010). The effect of the delivery of vascular endothelial growth factor and bone morphogenic protein-2 to osteoprogenitor cell populations on bone formation. *Biomaterials* 31, 1242–1250. doi:10.1016/j.biomaterials.2009.10.059

Karageorgiou, V., and Kaplan, D. (2005). Porosity of 3D biomaterial scaffolds and osteogenesis. *Biomaterials* 26, 5474–5491. doi:10.1016/j.biomaterials.2005.02.002

Khang, D., Choi, J., Im, Y.-M., Kim, Y.-J., Jang, J.-H., Kang, S. S., et al. (2012). Role of subnano-nano- and submicron-surface features on osteoblast differentiation of bone marrow mesenchymal stem cells. *Biomaterials* 33, 5997–6007. doi:10.1016/j.biomaterials.2012.05.005

Knychala, J., Bouropoulos, N., Catt, C. J., Katsamenis, O. L., Please, C. P., and Sengers, B. G. (2013). Pore geometry regulates early stage human bone marrow cell tissue formation and organisation. *Ann. Biomed. Eng.* 41, 917–930. doi:10.1007/s10439-013-0748-z

Kommareddy, K. P., Lange, C., Rumpler, M., Dunlop, J. W. C., Manjubala, I., Cui, J., et al. (2010). Two stages in three-dimensional *in vitro* growth of tissue generated by osteoblastlike cells. *Biointerphases* 5, 45–52. doi:10.1116/1.3431524

Kowalczewski, C. J., and Saul, J. M. (2018). Biomaterials for the delivery of growth factors and other therapeutic agents in tissue engineering approaches to bone regeneration. *Front. Pharmacol.* 9, 513. doi:10.3389/fphar.2018.00513

Kuhn, L. T., Peng, T., Gronowicz, G., and Hurley, M. M. (2021). Endogenous FGF -2 levels impact FGF -2/BMP -2 growth factor delivery dosing in aged murine calvarial bone defects. *J. Biomed. Mat. Res. A* 109, 2545–2555. doi:10.1002/jbm.a.37249

Lafon, J. P., Champion, E., and Bernache-Assollant, D. (2008). Processing of AB-type carbonated hydroxyapatite Ca10−x(PO4)6−x(CO3)x(OH)2−x−2y(CO3)y ceramics with controlled composition. *J. Eur. Ceram. Soc.* 28, 139–147. doi:10.1016/j.jeurceramsoc.2007.06.009

Lasgorceix, M., Champion, E., and Chartier, T. (2016). Shaping by microstereolithography and sintering of macro–micro-porous silicon substituted hydroxyapatite. *J. Eur. Ceram. Soc.* 36, 1091–1101. doi:10.1016/j.jeurceramsoc.2015.11.020

Lasgorceix, M., Costa, A. M., Mavropoulos, E., Sader, M., Calasans, M., Tanaka, M. N., et al. (2014). *In vitro* and *in vivo* evaluation of silicated hydroxyapatite and impact of insulin adsorption. *J. Mat. Sci. Mat. Med.* 25, 2383–2393. doi:10.1007/s10856-014-5237-x

Legros, R., Balmain, N., and Bonel, G. (1987). Age-related changes in mineral of rat and bovine cortical bone. *Calcif. Tissue Int.* 41, 137–144. doi:10.1007/BF02563793

Lerner, T., and Liljenqvist, U. (2013). Silicate-substituted calcium phosphate as a bone graft substitute in surgery for adolescent idiopathic scoliosis. *Eur. Spine J.* 22, 185–194. doi:10.1007/s00586-012-2485-7

Li, K., Xia, C., Qiao, Y., and Liu, X. (2019). Dose-response relationships between copper and its biocompatibility/antibacterial activities. *J. Trace Elem. Med. Biol.* 55, 127–135. doi:10.1016/j.jtemb.2019.06.015

Li, S., Wang, M., Chen, X., Li, S.-F., Li-Ling, J., and Xie, H.-Q. (2014). Inhibition of osteogenic differentiation of mesenchymal stem cells by copper supplementation. *Cell Prolif.* 47, 81–90. doi:10.1111/cpr.12083

Li, Y., Ho, J., and Ooi, C. P. (2010). Antibacterial efficacy and cytotoxicity studies of copper (II) and titanium (IV) substituted hydroxyapatite nanoparticles. *Mater. Sci. Eng. C* 30, 1137–1144. doi:10.1016/j.msec.2010.06.011

Lopes, D., Martins-Cruz, C., Oliveira, M. B., and Mano, J. F. (2018). Bone physiology as inspiration for tissue regenerative therapies. *Biomaterials* 185, 240–275. doi:10.1016/j.biomaterials.2018.09.028

Lowery, J. W., and Rosen, V. (2018). Bone morphogenetic protein–based therapeutic approaches. *Cold Spring Harb. Perspect. Biol.* 10, a022327. doi:10.1101/cshperspect.a022327

Magnaudeix, A., Usseglio, J., Lasgorceix, M., Lalloue, F., Damia, C., Brie, J., et al. (2016). Quantitative analysis of vascular colonisation and angio-conduction in porous silicon-substituted hydroxyapatite with various pore shapes in a chick chorioallantoic membrane (CAM) model. *Acta Biomater.* 38, 179–189. doi:10.1016/j.actbio.2016.04.039

Malmström, J., Adolfsson, E., Arvidsson, A., and Thomsen, P. (2007). Bone response inside free-form fabricated macroporous hydroxyapatite scaffolds with and without an open microporosity. *Clin. Implant Dent. Relat. Res.* 9, 79–88. doi:10.1111/j.1708-8208.2007.00031.x

Marchat, D., and Champion, E. (2017). "Ceramic devices for bone regeneration," in *Advances in ceramic biomaterials* (Elsevier), 279–311. doi:10.1016/B978-0-08-100881-2.00008-7

Masters, E. A., Ricciardi, B. F., Bentley, K. L. d. M., Moriarty, T. F., Schwarz, E. M., and Muthukrishnan, G. (2022). Skeletal infections: Microbial pathogenesis, immunity and clinical management. *Nat. Rev. Microbiol.* 20, 385–400. doi:10.1038/s41579-022-00686-0

Mercado-Pagán, Á. E., Stahl, A. M., Shanjani, Y., and Yang, Y. (2015). Vascularization in bone tissue engineering constructs. *Ann. Biomed. Eng.* 43, 718–729. doi:10.1007/s10439-015-1253-3

Nelson, C. M., Jean, R. P., Tan, J. L., Liu, W. F., Sniadecki, N. J., Spector, A. A., et al. (2005). Emergent patterns of growth controlled by multicellular form and mechanics. *Proc. Natl. Acad. Sci. U. S. A.* 102, 11594–11599. doi:10.1073/pnas.0502575102

O'Neill, E., Awale, G., Daneshmandi, L., Umerah, O., and Lo, K. W.-H. (2018). The roles of ions on bone regeneration. *Drug Discov. Today* 23, 879–890. doi:10.1016/j.drudis.2018.01.049

Ortali, C., Julien, I., Vandenhende, M., Drouet, C., and Champion, E. (2018). Consolidation of bone-like apatite bioceramics by spark plasma sintering of

amorphous carbonated calcium phosphate at very low temperature. *J. Eur. Ceram. Soc.* 38, 2098–2109. doi:10.1016/j.jeurceramsoc.2017.11.051

Othmani, M., Bachoua, H., Ghandour, Y., Aissa, A., and Debbabi, M. (2018). Synthesis, characterization and catalytic properties of copper-substituted hydroxyapatite nanocrystals. *Mater. Res. Bull.* 97, 560–566. doi:10.1016/j.materresbull.2017.09.056

Palard, M., Champion, E., and Foucaud, S. (2008). Synthesis of silicated hydroxyapatite Ca10(PO4)6−x(SiO4)x(OH)2−x. *J. Solid State Chem.* 181, 1950–1960. doi:10.1016/j.jssc.2008.04.027

Parent, M., Magnaudeix, A., Delebassée, S., Sarre, E., Champion, E., Viana Trecant, M., et al. (2016). Hydroxyapatite microporous bioceramics as vancomycin reservoir: Antibacterial efficiency and biocompatibility investigation. *J. Biomater. Appl.* 31, 488–498. doi:10.1177/0885328216653108

Pierschbacher, M. D., and Ruoslahti, E. (1984). Cell attachment activity of fibronectin can be duplicated by small synthetic fragments of the molecule. *Nature* 309, 30–33. doi:10.1038/309030a0

Pieters, I. Y., Van den Vreken, N. M. F., Declercq, H. A., Cornelissen, M. J., and Verbeeck, R. M. H. (2010). Carbonated apatites obtained by the hydrolysis of monetite: Influence of carbonate content on adhesion and proliferation of MC3T3-E1 osteoblastic cells. *Acta Biomater.* 6, 1561–1568. doi:10.1016/j.actbio.2009.11.002

Poli, E., Magnaudeix, A., Damia, C., Lalloué, F., Chaleix, V., Champion, E., et al. (2019). Advanced protocol to functionalize CaP bioceramic surface with peptide sequences and effect on murine pre-osteoblast cells proliferation. *Bioorg. Med. Chem. Lett.* 29, 1069–1073. doi:10.1016/j.bmcl.2019.03.002

Rao, R. R., Roopa, H. N., and Kannan, T. S. (1997). Solid state synthesis and thermal stability of HAP and HAP – β-TCP composite ceramic powders. *J. Mat. Sci. Mat. Med.* 8, 511–518. doi:10.1023/A:1018586412270

Ratanavaraporn, J., Furuya, H., Kohara, H., and Tabata, Y. (2011). Synergistic effects of the dual release of stromal cell-derived factor-1 and bone morphogenetic protein-2 from hydrogels on bone regeneration. *Biomaterials* 32, 2797–2811. doi:10.1016/j.biomaterials.2010.12.052

Ratnayake, J. T. B., Mucalo, M., and Dias, G. J. (2017). Substituted hydroxyapatites for bone regeneration: A review of current trends: Substituted HA for bone regeneration. *J. Biomed. Mat. Res.* 105, 1285–1299. doi:10.1002/jbm.b.33651

Raynaud, S., Champion, E., Bernache-Assollant, D., and Thomas, P. (2002). Calcium phosphate apatites with variable Ca/P atomic ratio I. Synthesis, characterisation and thermal stability of powders. *Biomaterials* 23, 1065–1072. doi:10.1016/S0142-9612(01)00218-6

Rey, C., Combes, C., Drouet, C., and Glimcher, M. J. (2009). Bone mineral: update on chemical composition and structure. *Osteoporos. Int.* 20, 1013–1021. doi:10.1007/s00198-009-0860-y

Rey, C., and Combes, C. (2016). "Physical chemistry of biological apatites," in *Biomineralization and biomaterials* (Elsevier), 95–127. doi:10.1016/B978-1-78242-338-6.00004-1

Ribatti, D. (2022). The chick embryo chorioallantoic membrane as an experimental model to study *in vivo* angiogenesis in glioblastoma multiforme. *Brain Res. Bull.* 182, 26–29. doi:10.1016/j.brainresbull.2022.02.005

Ribatti, D., Vacca, A., Roncali, L., and Dammacco, F. (2000). The chick embryo chorioallantoic membrane as a model for *in vivo* research on anti-angiogenesis. *Curr. Pharm. Biotechnol.* 1, 73–82. doi:10.2174/1389201003379040

Rosa, A. L., Beloti, M. M., and van Noort, R. (2003). Osteoblastic differentiation of cultured rat bone marrow cells on hydroxyapatite with different surface topography. *Dent. Mater.* 19, 768–772. doi:10.1016/S0109-5641(03)00024-1

Rotman, S. G., Sumrall, E., Ziadlou, R., Grijpma, D. W., Richards, R. G., Eglin, D., et al. (2020). Local bacteriophage delivery for treatment and prevention of bacterial infections. *Front. Microbiol.* 11, 538060. doi:10.3389/fmicb.2020.538060

Rüdrich, U., Lasgorceix, M., Champion, E., Pascaud-Mathieu, P., Damia, C., Chartier, T., et al. (2019). Pre-osteoblast cell colonization of porous silicon substituted hydroxyapatite bioceramics: Influence of microporosity and macropore design. *Mater. Sci. Eng. C* 97, 510–528. doi:10.1016/j.msec.2018.12.046

Rumpler, M., Woesz, A., Dunlop, J. W. C., van Dongen, J. T., and Fratzl, P. (2008). The effect of geometry on three-dimensional tissue growth. *J. R. Soc. Interface* 5, 1173–1180. doi:10.1098/rsif.2008.0064

Salhotra, A., Shah, H. N., Levi, B., and Longaker, M. T. (2020). Mechanisms of bone development and repair. *Nat. Rev. Mol. Cell Biol.* 21, 696–711. doi:10.1038/s41580-020-00279-w

Schamel, M., Bernhardt, A., Quade, M., Würkner, C., Gbureck, U., Moseke, C., et al. (2017). Cu2+, Co2+ and Cr3+ doping of a calcium phosphate cement influences materials properties and response of human mesenchymal stromal cells. *Mater. Sci. Eng. C* 73, 99–110. doi:10.1016/j.msec.2016.12.052

Schickle, K., Zurlinden, K., Bergmann, C., Lindner, M., Kirsten, A., Laub, M., et al. (2011). Synthesis of novel tricalcium phosphate-bioactive glass composite and functionalization with rhBMP-2. *J. Mat. Sci. Mat. Med.* 22, 763–771. doi:10.1007/s10856-011-4252-4

Schneiders, W., Reinstorf, A., Pompe, W., Grass, R., Biewener, A., Holch, M., et al. (2007). Effect of modification of hydroxyapatite/collagen composites with sodium citrate, phosphoserine, phosphoserine/RGD-peptide and calcium carbonate on bone remodelling. *Bone* 40, 1048–1059. doi:10.1016/j.bone.2006.11.019

Schorn, L., Sproll, C., Ommerborn, M., Naujoks, C., Kübler, N. R., and Depprich, R. (2017). Vertical bone regeneration using rhBMP-2 and VEGF. *Head. Face Med.* 13, 11. doi:10.1186/s13005-017-0146-0

Shanmugam, S., and Gopal, B. (2014). Copper substituted hydroxyapatite and fluorapatite: Synthesis, characterization and antimicrobial properties. *Ceram. Int.* 40, 15655–15662. doi:10.1016/j.ceramint.2014.07.086

Shen, X., Zhang, Y., Gu, Y., Xu, Y., Liu, Y., Li, B., et al. (2016). Sequential and sustained release of SDF-1 and BMP-2 from silk fibroin-nanohydroxyapatite scaffold for the enhancement of bone regeneration. *Biomaterials* 106, 205–216. doi:10.1016/j.biomaterials.2016.08.023

Simchi, A., Tamjid, E., Pishbin, F., and Boccaccini, A. R. (2011). Recent progress in inorganic and composite coatings with bactericidal capability for orthopaedic applications. *Nanomedicine Nanotechnol. Biol. Med.* 7, 22–39. doi:10.1016/j.nano.2010.10.005

Skoog, S. A., Kumar, G., Narayan, R. J., and Goering, P. L. (2018). Biological responses to immobilized microscale and nanoscale surface topographies. *Pharmacol. Ther.* 182, 33–55. doi:10.1016/j.pharmthera.2017.07.009

Šupová, M. (2015). Substituted hydroxyapatites for biomedical applications: A review. *Ceram. Int.* 41, 9203–9231. doi:10.1016/j.ceramint.2015.03.316

Szurkowska, K., and Kolmas, J. (2017). Hydroxyapatites enriched in silicon – bioceramic materials for biomedical and pharmaceutical applications. *Prog. Nat. Sci. Mater. Int.* 27, 401–409. doi:10.1016/j.pnsc.2017.08.009

Tang, G., Liu, Z., Liu, Y., Yu, J., Wang, X., Tan, Z., et al. (2021). Recent trends in the development of bone regenerative biomaterials. *Front. Cell Dev. Biol.* 9, 665813. doi:10.3389/fcell.2021.665813

Thomas, C. J., Mirza, R. G., and Gill, M. K. (2021). Age-related macular degeneration. *Med. Clin. N. Am.* 105, 473–491. doi:10.1016/j.mcna.2021.01.003

Tricard, J., Chermat, A., Balkhi, S. E., Denes, E., and Bertin, F. (2020). An antibiotic loaded ceramic sternum to treat destroyed infected sternum: 4 cases. *J. Thorac. Dis.* 12, 209–216. doi:10.21037/jtd.2020.01.70

Urish, K. L., and Cassat, J. E. (2020). *Staphylococcus aureus* osteomyelitis: Bone, bugs, and surgery. *Infect. Immun.* 88, e00932–19. doi:10.1128/IAI.00932-19

Walter, N., Baertl, S., Alt, V., and Rupp, M. (2021). What is the burden of osteomyelitis in Germany? An analysis of inpatient data from 2008 through 2018. *BMC Infect. Dis.* 21, 550. doi:10.1186/s12879-021-06274-6

Wang, W., and Yeung, K. W. K. (2017). Bone grafts and biomaterials substitutes for bone defect repair: A review. *Bioact. Mater.* 2, 224–247. doi:10.1016/j.bioactmat.2017.05.007

Wassif, R. K., Elkayal, M., Shamma, R. N., and Elkheshen, S. A. (2021). Recent advances in the local antibiotics delivery systems for management of osteomyelitis. *Drug Deliv.* 28, 2392–2414. doi:10.1080/10717544.2021.1998246

Zhang, J., Luo, X., Barbieri, D., Barradas, A. M. C., de Bruijn, J. D., van Blitterswijk, C. A., et al. (2014). The size of surface microstructures as an osteogenic factor in calcium phosphate ceramics. *Acta Biomater.* 10, 3254–3263. doi:10.1016/j.actbio.2014.03.021

Zhao, C., Liu, W., Zhu, M., Wu, C., and Zhu, Y. (2022). Bioceramic-based scaffolds with antibacterial function for bone tissue engineering: A review. *Bioact. Mater.* 18, 383–398. doi:10.1016/j.bioactmat.2022.02.010